Fuzzy Sampled-Data Control for Synchronization of T–S Fuzzy Reaction–Diffusion Neural Networks With Additive Time-Varying Delays

Ruimei Zhang, Deqiang Zeng, Ju H. Park, *Senior Member, IEEE*, Hak-Keung Lam, *Fellow, IEEE*, and Xiangpeng Xie, *Member, IEEE*

***Abstract*—This article focuses on the exponential synchronization problem of T–S fuzzy reaction–diffusion neural networks (RDNNs) with additive time-varying delays (ATVDs). Two control strategies, namely, fuzzy time sampled-data control and fuzzy time–space sampled-data control are newly proposed. Compared with some existing control schemes, the two fuzzy sampled-data control schemes cannot only tolerate some uncertainties but also save the limited communication resources for the considered systems. A new fuzzy-dependent adjustable matrix inequality technique is proposed. According to different fuzzy plant and controller rules, different adjustable matrices are introduced. In comparison with some traditional estimation techniques with a determined constant matrix, the fuzzy-dependent adjustable matrix approach is more flexible. Then, by constructing a suitable Lyapunov–Krasovskii functional (LKF) and using the fuzzy-dependent adjustable matrix approach, new exponential synchronization criteria are derived for T–S fuzzy RDNNs with ATVDs. Meanwhile, the desired fuzzy time and time–space sampled-data control gains are obtained by solving a set of linear matrix inequalities (LMIs). In the end, some simulations are presented to verify the effectiveness and superiority of the obtained theoretical results.**

***Index Terms*—Additive time-varying delays (ATVDs), exponential synchronization, fuzzy-dependent adjustable matrix inequality technique, fuzzy time sampled-data control, fuzzy time–space sampled-data control, T–S fuzzy reaction–diffusion neural networks (RDNNs).**

Manuscript received March 4, 2020; accepted May 18, 2020. Date of publication June 10, 2020; date of current version April 15, 2021. The work of Ju H. Park was supported by the National Research Foundation of Korea grant funded by the Korea Government (MSIT) under Grant 2020R1A2B5B02002002. The work of Xiangpeng Xie was supported by the Jiangsu Natural Science Foundation for Distinguished Young Scholars under Grant BK20190039. This article was recommended by Associate Editor C.-F. Juang. *(Corresponding author: Ju H. Park.)*

Ruimei Zhang is with the College of Cybersecurity, Sichuan University, Chengdu 610065, China (e-mail: ruimeizhang163@163.com).

Deqiang Zeng is with the School of Mathematics Sciences, Sichuan Normal University, Chengdu 610066, China (e-mail: zengdq22@163.com).

Ju H. Park is with the Department of Electrical Engineering, Yeungnam University, Gyeongsan 38541, South Korea (e-mail: jessie@ynu.ac.kr).

Hak-Keung Lam is with the Department of Engineering, King's College London, London WC2R 2LS, U.K. (e-mail: hak-keung.lam@kcl.ac.uk).

Xiangpeng Xie is with the Institute of Advanced Technology, Nanjing University of Posts and Telecommunications, Nanjing 210003, China (e-mail: xiexp@njupt.edu.cn).

Color versions of one or more figures in this article are available at https://doi.org/10.1109/TCYB.2020.2996619.

Digital Object Identifier 10.1109/TCYB.2020.2996619

I. Introduction

DURING the past decades, fuzzy control has provoked increasing interests of many researchers from various fields. Fuzzy control is regarded not only as a useful but also simple method to control many nonlinear complex systems, especially for systems or control processes with uncertainties [1]–[9]. For example, fuzzy control has been used to control two-wheeled robots in [4]. In [5], fuzzy control has been applied to stabilize the Rössler chaotic systems. In [6], the determination of the optimal green period ratios and traffic light cycle times have been realized by fuzzy control. In [7], fuzzy control has been applied to nonlinear networked systems. In [8], fuzzy control has been considered to solve the guaranteed cost control problem of uncertain stochastic fuzzy systems. In [9], fuzzy control has been used to solve the output tracking problem for T–S fuzzy systems with saturating actuators. Among diverse fuzzy control models, the T–S fuzzy model is one of the most popular ways to analyze and design fuzzy systems. Based on the T–S fuzzy model method, many T–S fuzzy systems have been diffusely investigated since they have substantial applications, such as the truck–trailer system [10], Mars entry vehicles [11], and so forth.

Recently, much attention has been paid to neural networks (NNs) due to their benefits in learning algorithms and handling data. As a result, extensive applications of NNs are found in a variety of areas, including financial market, image decryption, fixed-point computations, and signal processing [12]–[15]. As one of the most important dynamical behaviors of NNs, synchronization is in the spotlight. Synchronization is a universal phenomenon in many real systems and has considerable engineering applications in secure communication, biological systems, and mechatronic systems [16]–[18]. Thus, it is far reaching to study the synchronization of NNs.

In the existing literature, most of the NN models are built under the hypothesis that the interests of all neurons are evenly distributed. In fact, due to the influence of environmental factors, the reaction and diffusion phenomena inevitably exist in NNs. Therefore, it is meaningful to consider the spatial evolutions of NNs. Reaction–diffusion NNs (RDNNs), in which the neuron states are dependent on both time and space, can perfectly describe the time and spatial evolutions. In comparison with the traditional NNs, RDNNs could realize better approximations of actual systems. Until now, many interesting results on RDNNs are obtainable in [19]–[23]. For instance,

in [19], the impulsive synchronization problem of RDNNs has been investigated by an impulse-time-dependent LKF method. In [20], by constructing a new LKF with the neuron activation function information, stochastic synchronization has been considered for the Markovian RDNNs with actuator failures. In [23], by fuzzy control, the stabilization problem has been studied for T–S fuzzy RDNNs.

In the meantime, the time delay is often encountered in RDNNs because of the finite switching speeds of amplifiers and the congestions of signal transmission. The existence of time delay may cause oscillation or the instability to deteriorate the performance of RDNNs. It is, therefore, important to study RDNNs with time delay. Note that in the existing works of RDNNs [19]–[23], the time delay is considered as a single component in the state variables. In implementation, due to the different transmission conditions in the different segments of RDNNs, signals transmitted from one point to another may lead to additive time-varying delays (ATVDs) with different properties. Thus, it is necessary to consider ATVDs for RDNNs. However, to the best of our knowledge, the synchronization of T–S fuzzy RDNNs with ATVDs has not been considered, which is the first motivation of this article.

In order to realize the synchronization of RDNNs with time delays, various control strategies have been proposed, such as quantized feedback control [24], pinning impulsive control [25], and adaptive control [26]. With the development of communication and digital technologies, sampled-data control has stimulated increasing attention [27]–[29]. Based on sampled-data control, the synchronization of RDNNs has been extensively investigated [30]–[33]. For example, in [30], by time sampled-data control, the exponential synchronization problem has been studied for RDNNs with sampled-data communications. In [31], by spatial sampled-data control, the exponential synchronization of RDNNs with time delays has been investigated. In [33], by proposing a time sampled-data controller and a discontinuous LKF, synchronization criteria have been established for RDNNs with time delays. Although some new results for synchronization of RDNNs with sampled-data control have been presented in [33], a mistake occurs in $V_1(t)$ of the constructed LKF. The matrix dimensions of $V_1(t)$ are not matched because of $D_k \in \mathscr{R}^{n\times n}$ and $([\partial e_i(t,x)]/\partial x_k)^T \in \mathscr{R}^{1\times n}$. Moreover, in the existing works of RDNNs [30]–[33], all sampled-data control schemes are designed with the assumption that there is no uncertainty in control processes. In practice, due to the impact of environment and restrictions of equipment, uncertainties commonly exist in the control processes of RDNNs. Hence, it is profound in both theory and application to design a fuzzy sampled-data control scheme for RDNNs. However, few works have considered such a control scheme for synchronization of T–S fuzzy RDNNs with ATVDs.

Motivated by the above-mentioned discussions, by designing fuzzy time and time–space sampled-data control, we intend to study the exponential synchronization of T–S fuzzy RDNNs with ATVDs. The main contributions are highlighted as follows.

1) Two control strategies, which are fuzzy time sampled-data control and fuzzy time–space sampled-data control, are proposed for T–S fuzzy RDNNs. The two fuzzy sampled-data control schemes can not only tolerate some uncertainties but also save the limited communication resources of T–S fuzzy RDNNs.
2) A fuzzy-dependent adjustable matrix inequality technique is first proposed. Compared with some traditional estimation techniques with a determined constant matrix, the fuzzy-dependent adjustable matrix inequality technique is more flexible and helpful to reduce the conservatism.
3) The ATVDs are considered for T–S fuzzy RDNNs, which generalize the existing models of RDNNs with a single time-varying delay. So the present model here can satisfy broader application requirements.

Notations: Let $\mathrm{col}\{\cdots\}$ denote a column vector, $\mathrm{diag}\{\cdots\}$ denote a block-diagonal matrix, $\mathscr{R}^n$ denote the n-dimensional Euclidean space, and $\mathscr{R}^{n\times n}$ denote the set of $n\times n$ real matrices. I_n, 0_n, and $0_{n,m}$ represent $n\times n$ identity matrix, $n\times n$ and $n\times m$ zero matrices, respectively. $\mathrm{Sym}\{\mathcal{S}\} = \mathcal{S}^T + \mathcal{S}$. $C([-\varpi^*, 0]\times\mho, \mathscr{R}^n)$ represents all continuous functions from $[-\varpi^*, 0]\times\mho$ to $\mathscr{R}^n$. For $\phi(s,x)\in\mathscr{R}^n$, the norm is denoted by $\|\phi(s,x)\| = (\int_{\underline{\alpha}}^{\bar{\alpha}} \phi^T(s,x)\phi(s,x)dx)^{(1/2)}$.

II. Problem Formulation and Preliminaries

Based on the T–S fuzzy model method [34], the T–S fuzzy RDNN with two ATVDs is described as follows.

Plant Rule m: IF $\varsigma_1(t)$ is ϑ_1^m and ... and $\varsigma_p(t)$ is ϑ_p^m, THEN

$$\begin{aligned}\frac{\partial\varphi(t,x)}{\partial t} &= \mathcal{D}\frac{\partial^2\varphi(t,x)}{\partial x^2} - \mathcal{A}_m\varphi(t,x) + \mathcal{B}_m^{(1)}f(\varphi(t,x)) \\ &\quad + \mathcal{B}_m^{(2)}f(\varphi(t-\varpi_1(t)-\varpi_2(t),x)) + \urcorner(t) \\ \varphi(t,\underline{\alpha}) &= \varphi(t,\bar{\alpha}) = 0,\ \ t\in[t_0,+\infty) \\ \varphi(s+t_0,x) &= \phi(s,x)\in C\big(\big[-\varpi^*,0\big]\times\mho,\mathscr{R}^n\big)\end{aligned} \tag{1}$$

where $m \in \beth = \{1,2,\ldots,r\}$, r is the number of fuzzy rules, $\varsigma_1(t),\ldots,\varsigma_p(t)$ are the premise variables, and $\vartheta_1^m,\ldots,\vartheta_p^m$ are the fuzzy sets. x is the space variable belonging to $\mho = [\underline{\alpha},\bar{\alpha}]$, $\underline{\alpha}$ and $\bar{\alpha}$ are constants. $\varphi(t,x) = \mathrm{col}\{\varphi_1(t,x),\varphi_2(t,x),\ldots,\varphi_n(t,x)\}\in\mathscr{R}^n$ is the state vector with $\varphi_i(t,x)$ being the ith neuron at time t and in space x. $f(\varphi(t,x)) = \mathrm{col}\{f_1(\varphi_1(t,x)),\ldots,f_n(\varphi_n(t,x))\}\in\mathscr{R}^n$ stands for the neuron activation function. $\mathcal{D} = \mathrm{diag}\{d_1,d_2,\ldots,d_n\}\in\mathscr{R}^{n\times n}$, in which $d_i\geq 0$ represents the transmission diffusion coefficient along the ith neuron. $\mathcal{A}_m = \mathrm{diag}\{a_{m1},a_{m2},\ldots,a_{mn}\}\in\mathscr{R}^{n\times n}$ with $a_{mi}>0$. $\mathcal{B}_m^{(k)} = (b_{mij}^{(k)})_{n\times n}\in\mathscr{R}^{n\times n}$ $(k=1,2)$ are the connection weight matrices. $\urcorner(t) = \mathrm{col}\{\urcorner_1(t),\urcorner_2(t),\ldots,\urcorner_n(t)\}\in\mathscr{R}^n$ is the external input. The second and third equations are the Dirichlet boundary condition and initial condition, respectively. $\varpi_1(t)$ and $\varpi_2(t)$ are time-varying delays and satisfy $0\leq\varpi_1(t)\leq\varpi_1^*$, $\dot{\varpi}_1(t)\leq\mu_1$, $0\leq\varpi_2(t)\leq\varpi_2^*$, and $\dot{\varpi}_2(t)\leq\mu_2$, and $\varpi(t)\triangleq\varpi_1(t)+\varpi_2(t)$, $\varpi^*\triangleq\varpi_1^*+\varpi_2^*$, and $\mu\triangleq\mu_1+\mu_2$.

By employing the weighted average fuzzy blending approach, the overall T–S fuzzy RDNN with ATVDs can be

described as

$$\begin{aligned}\frac{\partial\varphi(t,x)}{\partial t}=&\sum_{m=1}^{r}\theta_m(\varsigma(t))\Big\{\mathcal{D}\frac{\partial^2\varphi(t,x)}{\partial x^2}-\mathcal{A}_m\varphi(t,x)\\&+\mathcal{B}_m^{(2)}f(\varphi(t-\varpi_1(t)-\varpi_2(t),x))\\&+\mathcal{B}_m^{(1)}f(\varphi(t,x))+\urcorner(t)\Big\}\\\varphi\big(t,\underline{\alpha}\big)=&\varphi(t,\bar{\alpha})=0,\ t\in[t_0,+\infty)\\\varphi(s+t_0,x)=&\phi(s,x)\in C\big(\big[-\varpi^*,0\big]\times\mho,\mathscr{R}^n\big)\end{aligned}\tag{2}$$

where $\varsigma(t)=\text{col}\{\varsigma_1(t),\ldots,\varsigma_p(t)\}$, $\theta_m(\varsigma(t))$ is the normalized membership function with

$$\theta_m(\varsigma(t))=\frac{\vartheta^m(\varsigma(t))}{\sum_{k=1}^{r}\vartheta^k(\varsigma(t))}\geq 0$$
$$\vartheta^m(\varsigma(t))=\prod_{l=1}^{p}\vartheta_l^m(\varsigma_l(t)),\quad\sum_{m=1}^{r}\theta_m(\varsigma(t))=1$$

and $\vartheta_l^m(\varsigma_l(t))$ means the membership grade of $\varsigma_l(t)$ in ϑ_l^m.

Viewing system (2) as the drive system, we introduce the response system as

$$\begin{aligned}\frac{\partial\sigma(t,x)}{\partial t}=&\sum_{m=1}^{r}\theta_m(\varsigma(t))\Big\{\mathcal{D}\frac{\partial^2\sigma(t,x)}{\partial x^2}-\mathcal{A}_m\sigma(t,x)\\&+\mathcal{B}_m^{(2)}f(\sigma(t-\varpi_1(t)-\varpi_2(t),x))\\&+\mathcal{B}_m^{(1)}f(\sigma(t,x))+\urcorner(t)+\mathcal{U}(t,x)\Big\}\end{aligned}\tag{3}$$

where $\sigma(t,\underline{\alpha})=\sigma(t,\bar{\alpha})=0,\ t\in[\tilde{t}_0,+\infty)$, $\sigma(s+\tilde{t}_0,x)=\tilde{\phi}(s,x)\in C([-\varpi^*,0]\times\mho,\mathscr{R}^n)$, and $\mathcal{U}(t,x)\in\mathscr{R}^n$ is the control input signal.

Denote the error signal $\eta(t,x)=\sigma(t,x)-\varphi(t,x)=\text{col}\{\eta_1(t,x),\eta_2(t,x),\ldots,\eta_n(t,x)\}$. From (2) and (3), one obtains the following error system as:

$$\begin{aligned}\frac{\partial\eta(t,x)}{\partial t}=&\sum_{m=1}^{r}\theta_m(\varsigma(t))\Big\{\mathcal{D}\frac{\partial^2\eta(t,x)}{\partial x^2}-\mathcal{A}_m\eta(t,x)\\&+\mathcal{B}_m^{(2)}\tilde{f}(\eta(t-\varpi_1(t)-\varpi_2(t),x))\\&+\mathcal{B}_m^{(1)}\tilde{f}(\eta(t,x))+\mathcal{U}(t,x)\Big\}\end{aligned}\tag{4}$$

where $\eta(t,\underline{\alpha})=\eta(t,\bar{\alpha})=0,\ t\in[t_0^*,+\infty)$, $\eta(s+t_0^*,x)=\phi^*(s,x)\in C([-\varpi^*,0]\times\mho,\mathscr{R}^n)$, and $\tilde{f}(\eta(t,x))=f(\sigma(t,x))-f(\varphi(t,x))$.

The following assumption and lemmas are needed to derive the main results.

Assumption 1: For any $z_1,z_2\in\mathscr{R}$, there exist scalars l_i^- and l_i^+ such that $f_i(\cdot)$ in (1) satisfies

$$l_i^-\leq\frac{f_i(z_1)-f_i(z_2)}{z_1-z_2}\leq l_i^+,\ z_1\neq z_2\ i=1,2,\ldots,n.$$

Lemma 1 [35]: For appropriate dimensional matrix $\mathscr{Y}>0$ and vector $g(z)$, the following inequality holds: $-\int_{y_1}^{y_2}g^T(z)\mathscr{Y}g(z)dz\leq(y_2-y_1)\chi^T(t)\mathscr{E}^T\mathscr{Y}^{-1}\mathscr{E}\chi(t)+2\chi^T(t)\mathscr{E}^T\int_{y_1}^{y_2}g(z)dz$, where the appropriate dimensional matrix $\mathscr{E}$ and vector $\chi(t)$ are independent on the integral variable.

Lemma 2 [36]: For $\mathscr{C}>0\in\mathscr{R}^{n\times n}$, and all functions $y\in C([\underline{\alpha},\bar{\alpha}],\mathscr{R}^n)$ with $y(\underline{\alpha})=0$ or $y(\bar{\alpha})=0$, the following inequality is true:

$$\frac{4\big(\bar{\alpha}-\underline{\alpha}\big)^2}{\pi^2}\int_{\underline{\alpha}}^{\bar{\alpha}}\frac{dy^T(x)}{dx}\mathscr{C}\frac{dy(x)}{dx}dx\geq\int_{\underline{\alpha}}^{\bar{\alpha}}y^T(x)\mathscr{C}y(x)dx.$$

Moreover, if $y(\underline{\alpha})=y(\bar{\alpha})=0$, one finds

$$\frac{\big(\bar{\alpha}-\underline{\alpha}\big)^2}{\pi^2}\int_{\underline{\alpha}}^{\bar{\alpha}}\frac{dy^T(x)}{dx}\mathscr{C}\frac{dy(x)}{dx}dx\geq\int_{\underline{\alpha}}^{\bar{\alpha}}y^T(x)\mathscr{C}y(x)dx.$$

Lemma 3 [37]: Let scalars $0<\delta_1<2\delta$. If there exists an absolutely continuous function $\mathscr{V}:[t_0-\epsilon,+\infty)\to[0,+\infty)$ satisfying $\dot{\mathscr{V}}(t)\leq-2\delta\mathscr{V}(t)+\delta_1\sup_{-\epsilon\leq\theta\leq0}\mathscr{V}(t+\theta),\quad t\geq t_0$, then $\mathscr{V}(t)\leq e^{-2\delta^*(t-t_0)}\sup_{-\epsilon\leq\theta\leq0}\mathscr{V}(t_0+\theta),\quad t\geq t_0$, where $\delta^*>0$ is a unique positive solution of $\delta^*=\delta-[(\delta_1e^{2\delta^*\epsilon})/2]$.

III. Main Results

In this section, we will investigate the exponential synchronization of T–S fuzzy RDNN with ATVDs via two different control schemes. First, by proposing a fuzzy time sampled-data control scheme and a new fuzzy-dependent adjustable matrix inequality technique, a novel exponential synchronization criterion is derived for the T–S fuzzy RDNNs (2) and (3). To show the superiority of the fuzzy-dependent adjustable matrix approach, an exponential synchronization criterion by a traditional method is given for comparison. Then, in order to further save the limited network communication resources, we design a fuzzy time–space sampled-data controller. Based on the fuzzy time–space sampled-data control scheme, new sufficient conditions are further derived to exponentially synchronize the T–S fuzzy RDNNs with ATVDs.

A. Fuzzy Time Sampled-Data Control for Exponential Synchronization of RDNNs With ATVDs

Let the time sampling sequence be $0=t_0<t_1<\cdots<t_p<\cdots$. The time sampling interval h_p satisfies the following condition:

$$0<h_p\triangleq t_{p+1}-t_p=h,\quad p=0,1,2,\ldots\tag{5}$$

where h is a positive constant.

In order to save the limited communication resources of RDNNs and tolerate some uncertainties in the designing process of the controller, according to the parallel-distributed compensation method [10], the fuzzy time sampled-data controller for rule j is given by the following.

Controller Rule j: IF $\varsigma_1(t)$ is ϑ_1^j and $\ldots$ and $\varsigma_p(t)$ is ϑ_p^j, THEN

$$\mathcal{U}(t,x)=\mathcal{K}_j\eta(t_p,x),\quad j\in\beth,\quad t\in\big[t_p,t_{p+1}\big)\tag{6}$$

where $\mathcal{K}_j\in\mathscr{R}^{n\times n}$ $(j\in\beth)$ are the gains to be designed. Then, the overall fuzzy time sampled-data controller is inferred by

$$\mathcal{U}(t,x)=\sum_{j=1}^{r}\theta_j\big(\varsigma(t_p)\big)\mathcal{K}_j\eta\big(t_p,x\big),\ j\in\beth,t\in\big[t_p,t_{p+1}\big).\tag{7}$$

Substituting (7) into (4), we find

$$\begin{aligned}\frac{\partial \eta(t,x)}{\partial t} &= \sum_{m=1}^{r}\sum_{j=1}^{r}\theta_m(\varsigma(t))\theta_j\big(\varsigma(t_p)\big)\\ &\quad\times\Big\{\mathcal{D}\frac{\partial^2\eta(t,x)}{\partial x^2}\\ &\qquad-\mathcal{A}_m\eta(t,x)+\mathcal{B}_m^{(1)}\tilde{f}(\eta(t,x))\\ &\qquad+\mathcal{B}_m^{(2)}\tilde{f}(\eta(t-\varpi_1(t)-\varpi_2(t),x))\\ &\qquad+\mathcal{K}_j\eta(t_p,x)\Big\},\ t\in\big[t_p,t_{p+1}\big)\\ \eta\big(t,\underline{\alpha}\big)&=\eta(t,\bar{\alpha})=0,\ t\in\big[t_0^*,+\infty\big)\\ \eta\big(s+t_0^*,x\big)&=\phi^*(s,x)\in C\big(\big[-\varpi^*,0\big]\times\mho,\mathscr{R}^n\big).\end{aligned}\tag{8}$$

Remark 1: In implementation, due to the impact of the environment and restrictions of equipment, uncertainties ubiquitously exist in the designing process of the controller. Note that the existing control methodologies in [24]–[26] and [30]–[33] are designed with an ideal hypothesis that there is no uncertainty in the designing process. Fuzzy control is commonly known as a useful method to present the control processes with uncertainties. Meanwhile, sampled-data control is more effective to save the communication resources of RDNNs in comparison with the control methods in [24]–[26]. Thus, the fuzzy time sampled-data controller is designed in (7) for exponential synchronization of T–S fuzzy RDNNs (2) and (3). Compared with the existing control schemes in [24]–[26] and [30]–[33], the fuzzy time sampled-data controller (7) is more effective to tolerate some uncertainties and save the limited communication resources of RDNNs.

Lemma 4: Let $y(t)$ be a different function $[c_1,c_2]\to\mathscr{R}^n$. For

$$\begin{cases}\text{Plant Rule } m:\text{ IF } \varsigma_1(t) \text{ is } \vartheta_1^m \text{ and}\cdots\text{and}\\ \qquad\qquad \varsigma_p(t) \text{ is } \vartheta_p^m\\ \text{Controller Rule } j:\text{ IF } \varsigma_1(t) \text{ is } \vartheta_1^j \text{ and}\cdots\text{and}\\ \qquad\qquad \varsigma_p(t) \text{ is } \vartheta_p^j\end{cases}$$

if there exists a symmetric matrix $\mathcal{Y}_{mj}\in\mathscr{R}^{n\times n}$ satisfying

$$\Lambda_{mj}=\begin{bmatrix}\mathcal{S}_1 & \mathcal{S}_2+\mathcal{Y}_{mj}\\ * & \mathcal{S}_3\end{bmatrix}>0,\ m,j\in\daleth$$

then the following inequality holds:

$$\begin{aligned}&-\int_{c_1}^{c_2}w^T(s)\Lambda w(s)ds\\ &\le\sum_{m=1}^{r}\sum_{j=1}^{r}\theta_m(\varsigma(t))\theta_j\big(\varsigma(t_p)\big)\\ &\quad\times\Big[2\chi^T(t)\mathcal{F}_{mj}^T\int_{c_1}^{c_2}w(s)ds\\ &\qquad+(c_2-c_1)\chi^T(t)\mathcal{F}_{mj}^T\Lambda_{mj}^{-1}\mathcal{F}_{mj}\chi(t)\\ &\qquad+y^T(c_2)\mathcal{Y}_{mj}y(c_2)-y^T(c_1)\mathcal{Y}_{mj}y(c_1)\Big]\end{aligned}\tag{9}$$

where $w(t)=\mathrm{col}\{\dot{y}(t),y(t)\}$, $\Lambda=\begin{bmatrix}\mathcal{S}_1 & \mathcal{S}_2\\ * & \mathcal{S}_3\end{bmatrix}$, $\mathcal{S}_i^T=\mathcal{S}_i\in\mathscr{R}^{n\times n}$ $(i=1,3)$, and any matrix $\mathcal{S}_2\in\mathscr{R}^{n\times n}$. Matrices $\mathcal{F}_{mj}$ $(m,j\in\daleth)$ and vector $\chi(t)$ are with appropriate dimensions.

Proof: For symmetric matrices $\mathcal{Y}_{mj}\in\mathscr{R}^{n\times n}$ $(m,j\in\daleth)$, one finds the following zero equality:

$$\begin{aligned}0&=\sum_{m=1}^{r}\sum_{j=1}^{r}\theta_m(\varsigma(t))\theta_j(\varsigma(t_p))\\ &\quad\times\Big[y^T(c_2)\mathcal{Y}_{mj}y(c_2)\\ &\qquad-y^T(c_1)\mathcal{Y}_{mj}y(c_1)-2\int_{c_1}^{c_2}y^T(s)\mathcal{Y}_{mj}\dot{y}(s)ds\Big].\end{aligned}\tag{10}$$

From (10) and Lemma 1, we have

$$\begin{aligned}&-\int_{c_1}^{c_2}w^T(s)\Lambda w(s)ds\\ &=\sum_{m=1}^{r}\sum_{j=1}^{r}\theta_m(\varsigma(t))\theta_j(\varsigma(t_p))\\ &\quad\times\Big[-\int_{c_1}^{c_2}w^T(s)\Lambda w(s)ds\\ &\qquad+y^T(c_2)\mathcal{Y}_{mj}y(c_2)-y^T(c_1)\mathcal{Y}_{mj}y(c_1)\\ &\qquad-2\int_{c_1}^{c_2}y^T(s)\mathcal{Y}_{mj}\dot{y}(s)ds\Big]\\ &=\sum_{m=1}^{r}\sum_{j=1}^{r}\theta_m(\varsigma(t))\theta_j\big(\varsigma(t_p)\big)\\ &\quad\times\Big[-\int_{c_1}^{c_2}w^T(s)\Lambda_{mj}w(s)ds\\ &\qquad+y^T(c_2)\mathcal{Y}_{mj}y(c_2)-y^T(c_1)\mathcal{Y}_{mj}y(c_1)\Big]\\ &\le\sum_{m=1}^{r}\sum_{j=1}^{r}\theta_m(\varsigma(t))\theta_j(\varsigma(t_p))\\ &\quad\times\Big[2\chi^T(t)\mathcal{F}_{mj}^T\int_{c_1}^{c_2}w(s)ds\\ &\qquad+(c_2-c_1)\chi^T(t)\mathcal{F}_{mj}^T\Lambda_{mj}^{-1}\mathcal{F}_{mj}\chi(t)+y^T(c_2)\mathcal{Y}_{mj}y(c_2)\\ &\qquad-y^T(c_1)\mathcal{Y}_{mj}y(c_1)\Big].\end{aligned}\tag{11}$$

This completes the proof. ∎

Remark 2: It is worth mentioning that the fuzzy-dependent adjustable matrix inequality technique in Lemma 4 is first proposed. According to a different fuzzy plant rule m and the controller rule j, different adjustable matrices $\mathcal{F}_{mj}$ and $\mathcal{Y}_{mj}$ are introduced in (9). Thus, compared with the traditional estimation technique in Lemma 1 [35] with a determined constant matrix, the fuzzy-dependent adjustable matrix inequality technique is more flexible.

Next, by constructing an appropriate LKF and using the fuzzy-dependent adjustable matrix inequality technique, a new synchronization criterion is derived for T–S fuzzy RDNNs (2) and (3). For simplicity, we denote $h(t)=t-t_p$, $\mathcal{L}^-=\mathrm{diag}\{l_1^-,l_2^-,\ldots,l_n^-\}$, $\mathcal{L}^+=\mathrm{diag}\{l_1^+,l_2^+,\ldots,l_n^+\}$, $\mathcal{I}_i=[0_{n,(i-1)n}\ \ I_n\ \ 0_{n,(10-i)n}]$ $(i=1,\ldots,10)$, $\xi_1(t,x)=\mathrm{col}\{\eta(t,x),\tilde{f}(\eta(t,x))\}$, $\xi_2(t,x)=\eta(t,x)-\eta(t_p,x)$, $z(t,x)=$

$\begin{cases} \frac{1}{h(t)}\int_{t_p}^{t}\eta(s,x)ds, & t\neq t_p, \\ \eta(t_p,x), & t=t_p, \end{cases}$, $\xi_3(t,x) = \mathrm{col}\{\eta(t_p,x), z(t,x)\}$, $\xi_4(t,x) = \mathrm{col}\{(\partial\eta(t,x)/\partial t), \eta(t,x)\}$, and

$$\zeta(t,x) = \mathrm{col}\Big\{\eta(t,x), \eta(t_p,x), \tilde{f}(\eta(t,x)), \frac{\partial\eta(t,x)}{\partial t}, z(t,x) \\ \eta(t-\varpi(t),x), \tilde{f}(\eta(t-\varpi(t),x)), \eta(t-\varpi_1(t),x) \\ \eta\big(t-\varpi_1^*,x\big), \eta\big(t-\varpi^*,x\big)\Big\}.$$

Theorem 1: Let scalars $\varpi_i^* \geq 0$, μ_i $(i=1,2)$, $h>0$, and $0<\delta_1<2\kappa<2\gamma_j$ be given. If there exist symmetric matrices $\mathcal{P}>0\in\mathscr{R}^{n\times n}$, $\mathcal{Q}_1>0\in\mathscr{R}^{n\times n}$, $\mathcal{Q}_2>0\in\mathscr{R}^{2n\times 2n}$, $\mathcal{H}_i>0\in\mathscr{R}^{n\times n}$ $(i=1,2)$, $\mathcal{R}_i>0\in\mathscr{R}^{n\times n}$ $(i=1,2)$, $\mathcal{W}>0\in\mathscr{R}^{2n\times 2n}$, and $\mathcal{S}=\begin{bmatrix}\mathcal{S}_1 & \mathcal{S}_2\\ * & \mathcal{S}_3\end{bmatrix}>0\in\mathscr{R}^{2n\times 2n}$, diagonal matrices $\mathcal{G}_{mj}^{(i)}>0\in\mathscr{R}^{n\times n}$ $(i=1,2)$, and any matrices $\mathcal{M}\in\mathscr{R}^{n\times n}$, $\mathcal{Y}_{mj}^{(i)}\in\mathscr{R}^{n\times n}$ $(i=1,2,3)$, $\mathcal{F}_{mj}\in\mathscr{R}^{2n\times 4n}$, and $\mathcal{K}_j^*\in\mathscr{R}^{n\times n}$, for any $m,j\in\mathfrak{I}$ satisfying $\mathcal{M}\mathcal{D}\geq 0$ and

$$\mathcal{R}_{mj}^{(1)} = \begin{bmatrix}\mathcal{R}_1 & \mathcal{Y}_{mj}^{(1)}\\ * & \mathcal{R}_1\end{bmatrix} \geq 0 \tag{12}$$

$$\mathcal{R}_{mj}^{(2)} = \begin{bmatrix}\mathcal{R}_2 & \mathcal{Y}_{mj}^{(2)}\\ * & \mathcal{R}_2\end{bmatrix} \geq 0 \tag{13}$$

$$\mathcal{S}_{mj} = \begin{bmatrix}\mathcal{S}_1 & \mathcal{S}_2+\mathcal{Y}_{mj}^{(3)}\\ * & \mathcal{S}_3\end{bmatrix} \geq 0 \tag{14}$$

$$\Psi(0;h,0) < 0 \tag{15}$$

$$\begin{bmatrix}\Psi(0;h,h) & e^{-2\kappa h}\Upsilon_3^T\mathcal{F}_{mj}^T\\ * & -\frac{1}{h}e^{-2\kappa h}\mathcal{S}_{mj}\end{bmatrix} < 0 \tag{16}$$

then the T–S fuzzy RDNNs (2) and (3) can achieve exponential synchronization under the fuzzy time sampled-data controller (7), where $\Psi(\varrho;h_p,h(t)) = \sum_{i=1}^{6}\Psi_i(\varrho;h_p,h(t))$ with

$$\begin{aligned}
&\Psi_1\big(\varrho;h_p,h(t)\big)\\
&= \mathrm{Sym}\big\{\mathcal{I}_1^T\mathcal{P}\mathcal{I}_4\big\} + 2\kappa\mathcal{I}_1^T\mathcal{P}\mathcal{I}_1 - \delta_1\mathcal{I}_2^T\mathcal{P}\mathcal{I}_2 + \mathcal{I}_1^T\mathcal{Q}_1\mathcal{I}_1\\
&\quad - (1-\mu_1)e^{-2\kappa\varpi_1^*}\mathcal{I}_8^T\mathcal{Q}_1\mathcal{I}_8 + \big[\mathcal{I}_1^T,\mathcal{I}_3^T\big]\mathcal{Q}_2\big[\mathcal{I}_1^T,\mathcal{I}_3^T\big]^T\\
&\quad - (1-\mu)e^{-2\kappa\varpi^*}\big[\mathcal{I}_6^T,\mathcal{I}_7^T\big]\mathcal{Q}_2\big[\mathcal{I}_6^T,\mathcal{I}_7^T\big]^T\\
&\quad + \mathcal{I}_1^T(\mathcal{H}_1+\mathcal{H}_2)\mathcal{I}_1 - e^{-2\kappa\varpi_1^*}\mathcal{I}_9^T\mathcal{H}_1\mathcal{I}_9\\
&\quad - e^{-2\kappa\varpi^*}\mathcal{I}_{10}^T\mathcal{H}_2\mathcal{I}_{10}\\
&\Psi_2\big(\varrho;h_p,h(t)\big)\\
&= \varpi_1^*\mathcal{I}_4^T\mathcal{R}_1\mathcal{I}_4 - \frac{e^{-2\kappa\varpi_1^*}}{\varpi_1^*}\Upsilon_1^T\mathcal{R}_{mj}^{(1)}\Upsilon_1 + \varpi^*\mathcal{I}_4^T\mathcal{R}_2\mathcal{I}_4\\
&\quad - \frac{e^{-2\kappa\varpi^*}}{\varpi^*}\Upsilon_2^T\mathcal{R}_{mj}^{(2)}\Upsilon_2,\\
&\Psi_3\big(\varrho;h_p,h(t)\big)\\
&= \left(\frac{\kappa h^2}{2}+h_p-2h(t)\right)\big[\mathcal{I}_2^T,\mathcal{I}_5^T\big]\mathcal{W}\big[\mathcal{I}_2^T,\mathcal{I}_5^T\big]^T\\
&\quad + \big(h_p-h(t)\big)\mathrm{Sym}\left\{\big[\mathcal{I}_2^T,\mathcal{I}_5^T\big]\mathcal{W}\begin{bmatrix}0\\ -\mathcal{I}_5+\mathcal{I}_1\end{bmatrix}\right\}\\
&\Psi_4\big(\varrho;h_p,h(t)\big)\\
&= \big(h_p-h(t)\big)\big[\mathcal{I}_4^T,\mathcal{I}_1^T\big]\mathcal{S}\big[\mathcal{I}_4^T,\mathcal{I}_1^T\big]^T + e^{-2\kappa h}\mathcal{I}_1^T\mathcal{Y}_{mj}^{(3)}\mathcal{I}_1\\
&\quad + e^{-2\kappa h}\mathrm{Sym}\left\{\Upsilon_3^T\mathcal{F}_{mj}^T\begin{bmatrix}\mathcal{I}_1-\mathcal{I}_2\\ h(t)\mathcal{I}_5\end{bmatrix}\right\}\\
&\quad + \varrho e^{-2\kappa h}h(t)\Upsilon_3^T\mathcal{F}_{mj}^T\mathcal{S}_{mj}^{-1}\mathcal{F}_{mj}\Upsilon_3 - e^{-2\kappa h}\mathcal{I}_2^T\mathcal{Y}_{mj}^{(3)}\mathcal{I}_2\\
&\Psi_5\big(\varrho;h_p,h(t)\big)\\
&= \mathrm{Sym}\Big\{\big(\mathcal{I}_3-\mathcal{L}^-\mathcal{I}_1\big)^T\mathcal{G}_{mj}^{(1)}\big(\mathcal{L}^+\mathcal{I}_1-\mathcal{I}_3\big)\Big\}\\
&\quad + \mathrm{Sym}\Big\{\big(\mathcal{I}_7-\mathcal{L}^-\mathcal{I}_6\big)^T\mathcal{G}_{mj}^{(2)}\big(\mathcal{L}^+\mathcal{I}_6-\mathcal{I}_7\big)\Big\}\\
&\Psi_6\big(\varrho;h_p,h(t)\big)\\
&= \mathrm{Sym}\Big\{\big(\mathcal{I}_4^T+\gamma_j\mathcal{I}_1^T\big)\mathcal{M}\Big(-\mathcal{I}_4-\mathcal{A}_m\mathcal{I}_1+\mathcal{B}_m^{(1)}\mathcal{I}_3+\mathcal{B}_m^{(2)}\mathcal{I}_7\Big)\Big\}\\
&\quad + \mathrm{Sym}\Big\{\big(\mathcal{I}_4^T+\gamma_j\mathcal{I}_1^T\big)\mathcal{K}_j^*\mathcal{I}_2\Big\} - \frac{2\big(\gamma_j-\kappa\big)\pi^2}{\big(\bar{\alpha}-\underline{\alpha}\big)^2}\mathcal{I}_1^T\mathcal{M}\mathcal{D}\mathcal{I}_1
\end{aligned}$$

and $\Upsilon_1=[(\mathcal{I}_1-\mathcal{I}_8)^T,(\mathcal{I}_8-\mathcal{I}_9)^T]^T$, $\Upsilon_2=[(\mathcal{I}_1-\mathcal{I}_6)^T,(\mathcal{I}_6-\mathcal{I}_{10})^T]^T$, and $\Upsilon_3=[\mathcal{I}_1^T,\mathcal{I}_2^T,\mathcal{I}_4^T,\mathcal{I}_5^T]^T$. In the meantime, the desired fuzzy time sampled-data controller gains are given as

$$\mathcal{K}_j = \mathcal{M}^{-1}\mathcal{K}_j^*. \tag{17}$$

Proof: For $t\in[t_p,t_{p+1})$, choose the following LKF for error T–S fuzzy RDNN (8):

$$\mathscr{V}(t) = \sum_{i=1}^{10}\mathscr{V}_i(t) \tag{18}$$

where

$$\begin{aligned}
\mathscr{V}_1(t) &= \int_{\underline{\alpha}}^{\bar{\alpha}}\eta^T(t,x)\mathcal{P}\eta(t,x)dx\\
\mathscr{V}_2(t) &= \int_{\underline{\alpha}}^{\bar{\alpha}}\frac{\partial\eta^T(t,x)}{\partial x}\mathcal{M}\mathcal{D}\frac{\partial\eta(t,x)}{\partial x}dx\\
\mathscr{V}_3(t) &= \int_{\underline{\alpha}}^{\bar{\alpha}}\int_{t-\varpi_1(t)}^{t}e^{2\kappa(s-t)}\eta^T(s,x)\mathcal{Q}_1\eta(s,x)dsdx\\
\mathscr{V}_4(t) &= \int_{\underline{\alpha}}^{\bar{\alpha}}\int_{t-\varpi(t)}^{t}e^{2\kappa(s-t)}\xi_1^T(s,x)\mathcal{Q}_2\xi_1(s,x)dsdx\\
\mathscr{V}_5(t) &= \int_{\underline{\alpha}}^{\bar{\alpha}}\int_{t-\varpi_1^*}^{t}e^{2\kappa(s-t)}\eta^T(s,x)\mathcal{H}_1\eta(s,x)dsdx\\
\mathscr{V}_6(t) &= \int_{\underline{\alpha}}^{\bar{\alpha}}\int_{t-\varpi^*}^{t}e^{2\kappa(s-t)}\eta^T(s,x)\mathcal{H}_2\eta(s,x)dsdx\\
\mathscr{V}_7(t) &= \int_{\underline{\alpha}}^{\bar{\alpha}}\int_{-\varpi_1^*}^{0}\int_{t+\beta}^{t}e^{2\kappa(s-t)}\frac{\partial\eta^T(s,x)}{\partial s}\mathcal{R}_1\frac{\partial\eta(s,x)}{\partial s}dsd\beta dx\\
\mathscr{V}_8(t) &= \int_{\underline{\alpha}}^{\bar{\alpha}}\int_{-\varpi^*}^{0}\int_{t+\beta}^{t}e^{2\kappa(s-t)}\frac{\partial\eta^T(s,x)}{\partial s}\mathcal{R}_2\frac{\partial\eta(s,x)}{\partial s}dsd\beta dx\\
\mathscr{V}_9(t) &= \big(h_p-h(t)\big)h(t)\int_{\underline{\alpha}}^{\bar{\alpha}}\xi_3^T(t,x)\mathcal{W}\xi_3(t,x)dx\\
\mathscr{V}_{10}(t) &= \big(h_p-h(t)\big)\int_{\underline{\alpha}}^{\bar{\alpha}}\int_{t_p}^{t}e^{2\kappa(s-t)}\xi_4^T(s,x)\mathcal{S}\xi_4(s,x)dsdx.
\end{aligned}$$

It is noted that $\mathscr{V}_i(t)$ $(i=1,2,\ldots,8)$ is continuous and $\mathscr{V}_i(t)$ $(i=9,10)$ vanish before and after t_p. Then, $\lim_{t\to t_p}\mathscr{V}(t)=\mathscr{V}(t_p)$, from which one derives that $\mathscr{V}(t)$ is continuous in time.

Calculating $\dot{\mathscr{V}}(t)$ along the trajectories of error T–S fuzzy RDNN (8), it yields

$$\dot{\mathscr{V}}_1(t) = 2\int_{\underline{\alpha}}^{\bar{\alpha}}\eta^T(t,x)\mathcal{P}\frac{\partial\eta(t,x)}{\partial t}dx \tag{19}$$

$$\dot{\mathscr{V}}_2(t) = 2\int_{\underline{\alpha}}^{\bar{\alpha}} \frac{\partial^2 \eta^T(t,x)}{\partial x \partial t}\mathcal{M}\mathcal{D}\frac{\partial \eta(t,x)}{\partial x}dx \tag{20}$$

$$\begin{aligned}\dot{\mathscr{V}}_3(t) \le\ & -2\kappa\mathscr{V}_3(t) + \int_{\underline{\alpha}}^{\bar{\alpha}} \eta^T(t,x)\mathcal{Q}_1\eta(t,x)dx - (1-\mu_1)\\ & \times e^{-2\kappa\varpi_1^*}\int_{\underline{\alpha}}^{\bar{\alpha}} \eta^T(t-\varpi_1(t),x)\mathcal{Q}_1\eta(t-\varpi_1(t),x)dx\end{aligned} \tag{21}$$

$$\begin{aligned}\dot{\mathscr{V}}_4(t) \le\ & -2\kappa\mathscr{V}_4(t) + \int_{\underline{\alpha}}^{\bar{\alpha}} \xi_1^T(t,x)\mathcal{Q}_2\xi_1(t,x)dx - (1-\mu)\\ & \times e^{-2\kappa\varpi^*}\int_{\underline{\alpha}}^{\bar{\alpha}} \xi_1^T(t-\varpi(t),x)\mathcal{Q}_2\xi_1(t-\varpi(t),x)dx\end{aligned} \tag{22}$$

$$\begin{aligned}\dot{\mathscr{V}}_5(t) =\ & -2\kappa\mathscr{V}_5(t) + \int_{\underline{\alpha}}^{\bar{\alpha}} \eta^T(t,x)\mathcal{H}_1\eta(t,x)dx\\ & - e^{-2\kappa\varpi_1^*}\int_{\underline{\alpha}}^{\bar{\alpha}} \eta^T\big(t-\varpi_1^*,x\big)\mathcal{H}_1\eta\big(t-\varpi_1^*,x\big)dx\end{aligned} \tag{23}$$

$$\begin{aligned}\dot{\mathscr{V}}_6(t) =\ & -2\kappa\mathscr{V}_6(t) + \int_{\underline{\alpha}}^{\bar{\alpha}} \eta^T(t,x)\mathcal{H}_2\eta(t,x)dx\\ & - e^{-2\kappa\varpi^*}\int_{\underline{\alpha}}^{\bar{\alpha}} \eta^T\big(t-\varpi^*,x\big)\mathcal{H}_2\eta\big(t-\varpi^*,x\big)dx\end{aligned} \tag{24}$$

$$\begin{aligned}\dot{\mathscr{V}}_7(t) \le\ & -2\kappa\mathscr{V}_7(t) + \varpi_1^*\int_{\underline{\alpha}}^{\bar{\alpha}} \frac{\partial \eta^T(t,x)}{\partial t}\mathcal{R}_1\frac{\partial \eta(t,x)}{\partial t}dx\\ & - e^{-2\kappa\varpi_1^*}\int_{\underline{\alpha}}^{\bar{\alpha}}\int_{t-\varpi_1^*}^{t} \frac{\partial \eta^T(s,x)}{\partial s}\mathcal{R}_1\frac{\partial \eta(s,x)}{\partial s}dsdx\end{aligned} \tag{25}$$

$$\begin{aligned}\dot{\mathscr{V}}_8(t) \le\ & -2\kappa\mathscr{V}_8(t) + \varpi^*\int_{\underline{\alpha}}^{\bar{\alpha}} \frac{\partial \eta^T(t,x)}{\partial t}\mathcal{R}_2\frac{\partial \eta(t,x)}{\partial t}dx\\ & - e^{-2\kappa\varpi^*}\int_{\underline{\alpha}}^{\bar{\alpha}}\int_{t-\varpi^*}^{t} \frac{\partial \eta^T(s,x)}{\partial s}\mathcal{R}_2\frac{\partial \eta(s,x)}{\partial s}dsdx\end{aligned} \tag{26}$$

$$\begin{aligned}\dot{\mathscr{V}}_9(t) =\ & (h_p - 2h(t))\int_{\underline{\alpha}}^{\bar{\alpha}} \xi_3^T(t,x)\mathcal{W}\xi_3(t,x)dx\\ & + 2(h_p - h(t))\int_{\underline{\alpha}}^{\bar{\alpha}} \xi_3^T(t,x)\mathcal{W}\\ & \times \begin{bmatrix} 0 \\ -z(t,x)+\eta(t,x)\end{bmatrix}dx\end{aligned} \tag{27}$$

$$\begin{aligned}\dot{\mathscr{V}}_{10}(t) =\ & -2\kappa\mathscr{V}_{10}(t) - e^{-2\kappa h}\int_{\underline{\alpha}}^{\bar{\alpha}}\int_{t_p}^{t} \xi_4^T(s,x)\mathcal{S}\xi_4(s,x)dsdx\\ & + \big(h_p - h(t)\big)\int_{\underline{\alpha}}^{\bar{\alpha}} \xi_4^T(t,x)\mathcal{S}\xi_4(t,x)dx.\end{aligned} \tag{28}$$

According to Jensen's inequality [38] and reciprocally convex inequality [39], one has from (12) and (25) that

$$\begin{aligned}& -e^{-2\kappa\varpi_1^*}\int_{\underline{\alpha}}^{\bar{\alpha}}\int_{t-\varpi_1^*}^{t} \frac{\partial \eta^T(s,x)}{\partial s}\mathcal{R}_1\frac{\partial \eta(s,x)}{\partial s}dsdx\\ &= -e^{-2\kappa\varpi_1^*}\int_{\underline{\alpha}}^{\bar{\alpha}}\int_{t-\varpi_1(t)}^{t} \frac{\partial \eta^T(s,x)}{\partial s}\mathcal{R}_1\frac{\partial \eta(s,x)}{\partial s}dsdx\\ &\quad -e^{-2\kappa\varpi_1^*}\int_{\underline{\alpha}}^{\bar{\alpha}}\int_{t-\varpi_1^*}^{t-\varpi_1(t)} \frac{\partial \eta^T(s,x)}{\partial s}\mathcal{R}_1\frac{\partial \eta(s,x)}{\partial s}dsdx\\ &\le -\frac{e^{-2\kappa\varpi_1^*}}{\varpi_1^*}\sum_{m=1}^{r}\sum_{j=1}^{r}\theta_m(\varsigma(t))\theta_j\big(\varsigma(t_p)\big)\int_{\underline{\alpha}}^{\bar{\alpha}}\begin{bmatrix}\xi_6(t,x)\\ \xi_7(t,x)\end{bmatrix}^T\\ &\quad\times \mathcal{R}_{mj}^{(1)}\begin{bmatrix}\xi_6(t,x)\\ \xi_7(t,x)\end{bmatrix}dx\end{aligned} \tag{29}$$

where $\xi_6(t,x) = \eta(t,x) - \eta(t-\varpi_1(t),x)$ and $\xi_7(t,x) = \eta(t-\varpi_1(t),x) - \eta(t-\varpi_1^*,x)$.

Similarly, we have from (13) and (26)

$$\begin{aligned}& -e^{-2\kappa\varpi^*}\int_{\underline{\alpha}}^{\bar{\alpha}}\int_{t-\varpi^*}^{t} \frac{\partial \eta^T(s,x)}{\partial s}\mathcal{R}_2\frac{\partial \eta(s,x)}{\partial s}dsdx\\ &\le -\frac{e^{-2\kappa\varpi^*}}{\varpi^*}\sum_{m=1}^{r}\sum_{j=1}^{r}\theta_m(\varsigma(t))\theta_j\big(\varsigma(t_p)\big)\int_{\underline{\alpha}}^{\bar{\alpha}}\begin{bmatrix}\xi_8(t,x)\\ \xi_9(t,x)\end{bmatrix}^T\\ &\quad\times \mathcal{R}_{mj}^{(2)}\begin{bmatrix}\xi_8(t,x)\\ \xi_9(t,x)\end{bmatrix}dx\end{aligned} \tag{30}$$

where $\xi_8(t,x) = \eta(t,x) - \eta(t-\varpi(t),x)$ and $\xi_9(t,x) = \eta(t-\varpi(t),x) - \eta(t-\varpi^*,x)$.

From (14), (28), and Lemma 4, one can obtain

$$\begin{aligned}& -e^{-2\kappa h}\int_{\underline{\alpha}}^{\bar{\alpha}}\int_{t_p}^{t} \xi_4^T(s,x)\mathcal{S}\xi_4(s,x)dsdx\\ &\le \int_{\underline{\alpha}}^{\bar{\alpha}}\sum_{m=1}^{r}\sum_{j=1}^{r}\theta_m(\varsigma(t))\theta_j\big(\varsigma(t_p)\big)e^{-2\kappa h}\\ &\quad\times\Bigg[2\chi^T(t)\mathcal{F}_{mj}^T\times\begin{bmatrix}\xi_2(t,x)\\ h(t)z(t,x)\end{bmatrix}\\ &\qquad + h(t)\chi^T(t)\mathcal{F}_{mj}^T\mathcal{S}_{mj}^{-1}\mathcal{F}_{mj}\chi(t)\\ &\qquad + \eta^T(t,x)\mathcal{Y}_{mj}^{(3)}\eta(t,x) - \eta^T(t_p,x)\mathcal{Y}_{mj}^{(3)}\eta(t_p,x)\Bigg]dx\end{aligned} \tag{31}$$

where $\chi(t) = \mathrm{col}\{\eta(t,x),\ \eta(t_p,x), (\partial\eta(t,x)/\partial t), z(t,x)\}$.

By Assumption 1, for any diagonal matrices $\mathcal{G}_{mj}^{(k)} > 0 \in \mathscr{R}^{n\times n}(k=1,2; m,j\in\mathfrak{I})$, one obtains

$$\begin{aligned}& 2\sum_{m=1}^{r}\sum_{j=1}^{r}\theta_m(\varsigma(t))\theta_j\big(\varsigma(t_p)\big)\Big(\tilde{f}(\eta(t,x)) - \mathcal{L}^-\eta(t,x)\Big)^T\\ &\quad\times \mathcal{G}_{mj}^{(1)}\Big(\mathcal{L}^+\eta(t,x) - \tilde{f}(\eta(t,x))\Big) \ge 0\end{aligned} \tag{32}$$

$$\begin{aligned}& 2\sum_{m=1}^{r}\sum_{j=1}^{r}\theta_m(\varsigma(t))\theta_j\big(\varsigma(t_p)\big)\\ &\quad\times\Big(\tilde{f}(\eta(t-\varpi(t),x))\\ &\qquad - \mathcal{L}^-\eta(t-\varpi(t),x)\Big)^T\mathcal{G}_{mj}^{(2)}\big(\mathcal{L}^+\eta(t-\varpi(t),x)\\ &\qquad - \tilde{f}(\eta(t-\varpi(t),x))\Big) \ge 0.\end{aligned} \tag{33}$$

For any matrix $\mathcal{M}\in\mathscr{R}^{n\times n}$, one has from system (8) that

$$\begin{aligned}0 =\ & 2\int_{\underline{\alpha}}^{\bar{\alpha}}\sum_{m=1}^{r}\sum_{j=1}^{r}\theta_m(\varsigma(t))\theta_j\big(\varsigma(t_p)\big)\Big(\frac{\partial\eta(t,x)}{\partial t} + \gamma_j\eta(t,x)\Big)^T\\ &\times\Bigg[\mathcal{M}\Big(-\frac{\partial\eta(t,x)}{\partial t} + \mathcal{D}\frac{\partial^2\eta(t,x)}{\partial x^2} - \mathcal{A}_m\eta(t,x)\end{aligned}$$

$$+ \mathcal{B}_m^{(1)}\tilde{f}(\eta(t,x)) + \mathcal{B}_m^{(2)}\tilde{f}(\eta(t-\varpi(t),x))\Big) + \mathcal{K}_j^*\eta(t_p,x)\Big]dx \tag{34}$$

where $\mathcal{K}_j^* = \mathcal{M}\mathcal{K}_j$.

By the Dirichlet boundary condition in (8), integration by parts, and (34), one finds

$$\begin{aligned} 2\int_{\underline{\alpha}}^{\bar{\alpha}} \frac{\partial\eta^T(t,x)}{\partial t}\mathcal{M}\mathcal{D}\frac{\partial\eta^2(t,x)}{\partial x^2}dx &= 2\frac{\partial\eta^T(t,x)}{\partial t}\mathcal{M}\mathcal{D}\frac{\partial\eta(t,x)}{\partial x}\Big|_{x=\underline{\alpha}}^{x=\bar{\alpha}} \\ &\quad - 2\int_{\underline{\alpha}}^{\bar{\alpha}} \frac{\partial^2\eta^T(t,x)}{\partial x\partial t}\mathcal{M}\mathcal{D}\frac{\partial\eta(t,x)}{\partial x}dx \\ &= -2\int_{\underline{\alpha}}^{\bar{\alpha}} \frac{\partial^2\eta^T(t,x)}{\partial x\partial t}\mathcal{M}\mathcal{D}\frac{\partial\eta(t,x)}{\partial x}dx \end{aligned} \tag{35}$$

and

$$\begin{aligned} 2\gamma_j\int_{\underline{\alpha}}^{\bar{\alpha}} \eta^T(t,x)\mathcal{M}\mathcal{D}\frac{\partial\eta^2(t,x)}{\partial x^2}dx &= -2\gamma_j\int_{\underline{\alpha}}^{\bar{\alpha}} \frac{\partial\eta^T(t,x)}{\partial x}\mathcal{M}\mathcal{D}\frac{\partial\eta(t,x)}{\partial x}dx. \end{aligned} \tag{36}$$

From (36) and Lemma 2, one finds that

$$\begin{aligned} &2\kappa\mathcal{V}_2(t) - 2\gamma_j\int_{\underline{\alpha}}^{\bar{\alpha}} \frac{\partial\eta^T(t,x)}{\partial x}\mathcal{M}\mathcal{D}\frac{\partial\eta(t,x)}{\partial x}dx \\ &= -2\big(\gamma_j-\kappa\big)\int_{\underline{\alpha}}^{\bar{\alpha}} \frac{\partial\eta^T(t,x)}{\partial x}\mathcal{M}\mathcal{D}\frac{\partial\eta(t,x)}{\partial x}dx \\ &\le -\frac{2\big(\gamma_j-\kappa\big)\pi^2}{\big(\bar{\alpha}-\underline{\alpha}\big)^2}\int_{\underline{\alpha}}^{\bar{\alpha}} \eta^T(t,x)\mathcal{M}\mathcal{D}\eta(t,x)dx. \end{aligned} \tag{37}$$

Combining (19)–(37), we have for $t_p \le t < t_{p+1}$

$$\begin{aligned} &\dot{\mathcal{V}}(t) + 2\kappa\mathcal{V}(t) - \delta_1 \sup_{-\varpi^*\le s\le 0} \mathcal{V}(t+s) \\ &\le \int_{\underline{\alpha}}^{\bar{\alpha}} \sum_{m=1}^{r}\sum_{j=1}^{r}\theta_m(\varsigma(t))\theta_j\big(\varsigma(t_p)\big)\zeta^T(t,x) \\ &\quad\times \big(\Psi(1;h_p,h(t)) + \delta_1\mathcal{I}_2^T\mathcal{P}\mathcal{I}_2\big)\zeta(t,x)dx \\ &\quad - \delta_1\mathcal{V}_1(t_p) \\ &= \int_{\underline{\alpha}}^{\bar{\alpha}} \sum_{m=1}^{r}\sum_{j=1}^{r}\theta_m(\varsigma(t))\theta_j\big(\varsigma(t_p)\big)\zeta^T(t,x) \\ &\quad\times \Psi\big(1;h_p,h(t)\big)\zeta(t,x)dx \\ &= \int_{\underline{\alpha}}^{\bar{\alpha}} \sum_{m=1}^{r}\sum_{j=1}^{r}\theta_m(\varsigma(t))\theta_j(\varsigma(t_p))\zeta^T(t,x) \\ &\quad\times \left[\frac{h-h(t)}{h}\Psi(1;h,0) + \frac{h(t)}{h}\Psi(1;h,h)\right]\zeta(t,x)dx. \end{aligned} \tag{38}$$

Using the Schur complement to (16), for $\zeta(t,x) \ne 0$, one obtains from (15), (16), and (38) that for $t_p \le t < t_{p+1}$

$$\dot{\mathcal{V}}(t) + 2\kappa\mathcal{V}(t) - \delta_1 \sup_{-\varpi^*\le s\le 0} \mathcal{V}(t+s) < 0. \tag{39}$$

According to Lemma 3, we can obtain from (39) that $\mathcal{V}(t) \le e^{-2\delta^*(t-t_0)}\mathcal{V}(t_0)$. Then, we can conclude that the T–S fuzzy RDNN (2) is exponentially synchronized with (3) under the fuzzy time sampled-data controller (7). This completes the proof. ■

Remark 3: Based on the Lyapunov stability theory, choosing an appropriate LKF is crucial for deriving stability criteria. In this article, (18) is chosen as the LKF. $V_1(t)$ is the basic term. $V_2(t)$ is constructed to counteract the reaction–diffusion term $2\int_{\underline{\alpha}}^{\bar{\alpha}}[(\partial\eta^T(t,x))/\partial t]\mathcal{M}\mathcal{D}[(\partial\eta^2(t,x))/\partial x^2]dx$ in (34). It is well known that delay information and sampling information are effective to reduce the conservatism of stability criteria. In line with this, $V_i(t)$ $(i = 3,4,\ldots,8)$ are introduced to capture the information of the time delays $\varpi_1(t)$ and $\varpi_2(t)$ [if only single delay is considered, for example, $\varpi_1(t)$, then $V_i(t)$ $(i = 4,6,8)$ do not needed]. $V_i(t)$ $(i = 9,10)$ are used to capture the information of sampling.

Remark 4: It is noted that the fuzzy-dependent matrices $\mathcal{R}_{mj}^{(k)}$ $(k = 1,2)$, $\mathcal{S}_{mj}$, $\mathcal{Y}_{mj}^{(3)}$, $\mathcal{F}_{mj}$, and $\mathcal{G}_{mj}^{(k)}$ $(k = 1,2)$ are introduced in (29)–(33). It means that different matrices are chosen for different plant and controller rules, which effectively improve the feasible region of the synchronization conditions in Theorem 1.

To show the superiority of the fuzzy-dependent adjustable matrix approach, the following corollary by the traditional estimation technique in Lemma 1 [35] is given for comparison. Replace the fuzzy-dependent matrices $\mathcal{R}_{mj}^{(k)}$ $(k = 1,2)$, $\mathcal{F}_{mj}$, and $\mathcal{G}_{mj}^{(k)}$ $(k = 1,2)$ by constant matrices $\mathcal{R}^{(k)}$ $(k = 1,2)$, $\mathcal{F}$, and $\mathcal{G}^{(k)}$ $(k = 1,2)$. If the traditional estimation technique in Lemma 1 [35] is used to estimate $-e^{-2\kappa h}\int_{\underline{\alpha}}^{\bar{\alpha}}\int_{t_p}^{t}\xi_4^T(s,x)\mathcal{S}\xi_4(s,x)dsdx$, then (31) is changed into

$$\begin{aligned} &-e^{-2\kappa h}\int_{\underline{\alpha}}^{\bar{\alpha}}\int_{t_p}^{t}\xi_4^T(s,x)\mathcal{S}\xi_4(s,x)dsdx \\ &\le e^{-2\kappa h}\Bigg[h(t)\times\chi^T(t)\mathcal{F}^T\mathcal{S}^{-1}\mathcal{F}\chi(t) \\ &\qquad + 2\chi^T(t)\mathcal{F}^T\begin{bmatrix}\xi_2(t,x)\\ h(t)z(t,x)\end{bmatrix}\Bigg]dx. \end{aligned} \tag{40}$$

Then, from Theorem 1, we have the following corollary.

Corollary 1: Let scalars $\varpi_i^* \ge 0$, μ_i $(i = 1,2)$, $h > 0$, and $0 < \delta_1 < 2\kappa < 2\gamma_j$ be given. If there exist symmetric matrices $\mathcal{P} > 0 \in \mathscr{R}^{n\times n}$, $\mathcal{Q}_1 > 0 \in \mathscr{R}^{n\times n}$, $\mathcal{Q}_2 > 0 \in \mathscr{R}^{2n\times 2n}$, $\mathcal{H}_i > 0 \in \mathscr{R}^{n\times n}$ $(i = 1,2)$, $\mathcal{R}_i > 0 \in \mathscr{R}^{n\times n}$ $(i = 1,2)$, $\mathcal{W} > 0 \in \mathscr{R}^{2n\times 2n}$, and $\mathcal{S} = \begin{bmatrix}\mathcal{S}_1 & \mathcal{S}_2\\ * & \mathcal{S}_3\end{bmatrix} > 0 \in \mathscr{R}^{2n\times 2n}$, diagonal matrices $\mathcal{G}^{(i)} > 0 \in \mathscr{R}^{n\times n}$ $(i = 1,2)$, and any matrices $\mathcal{M} \in \mathscr{R}^{n\times n}$, $\mathcal{Y}^{(i)} \in \mathscr{R}^{n\times n}$ $(i = 1,2)$, $\mathcal{F} \in \mathscr{R}^{2n\times 4n}$, and $\mathcal{K}_j^* \in \mathscr{R}^{n\times n}$, for any $m, j \in \mathcal{I}$ satisfying $\mathcal{M}\mathcal{D} \ge 0$ and

$$\mathcal{R}^{(1)} = \begin{bmatrix}\mathcal{R}_1 & \mathcal{Y}^{(1)}\\ * & \mathcal{R}_1\end{bmatrix} \ge 0 \tag{41}$$

$$\mathcal{R}^{(2)} = \begin{bmatrix}\mathcal{R}_2 & \mathcal{Y}^{(2)}\\ * & \mathcal{R}_2\end{bmatrix} \ge 0 \tag{42}$$

$$\Psi^*(0;h,0) < 0 \tag{43}$$

$$\begin{bmatrix}\Psi^*(0;h,h) & e^{-2\kappa h}\Upsilon_3^T\mathcal{F}^T\\ * & -\frac{1}{h}e^{-2\kappa h}\mathcal{S}\end{bmatrix} < 0 \tag{44}$$

then the T–S fuzzy RDNNs (2) and (3) can achieve exponential synchronization under the fuzzy time sampled-data controller (7), where $\Psi^*(\varrho; h_p, h(t)) = \sum_{i=1,3,6} \Psi_i(\varrho; h_p, h(t)) \sum_{i=2,4,5} \Psi_i^*(\varrho; h_p, h(t))$ with

$$\begin{aligned}
&\Psi_2^*\big(\varrho; h_p, h(t)\big) \\
&= \varpi_1^* \mathcal{I}_4^T \mathcal{R}_1 \mathcal{I}_4 - \frac{e^{-2\kappa\varpi_1^*}}{\varpi_1^*} \Upsilon_1^T \mathcal{R}^{(1)} \Upsilon_1 + \varpi^* \mathcal{I}_4^T \mathcal{R}_2 \mathcal{I}_4 \\
&\quad - \frac{e^{-2\kappa\varpi^*}}{\varpi^*} \Upsilon_2^T \mathcal{R}^{(2)} \Upsilon_2, \\
&\Psi_4^*\big(\varrho; h_p, h(t)\big) \\
&= \big(h_p - h(t)\big)\big[\mathcal{I}_4^T, \mathcal{I}_1^T\big] \mathcal{S} \big[\mathcal{I}_4^T, \mathcal{I}_1^T\big]^T \\
&\quad + e^{-2\kappa h} \mathrm{Sym}\left\{ \Upsilon_3^T \mathcal{F}^T \begin{bmatrix} \mathcal{I}_1 - \mathcal{I}_2 \\ h(t)\mathcal{I}_5 \end{bmatrix} \right\} \\
&\quad + \varrho e^{-2\kappa h} h(t) \Upsilon_3^T \mathcal{F}^T \mathcal{S}^{-1} \mathcal{F} \Upsilon_3 \\
&\Psi_5^*\big(\varrho; h_p, h(t)\big) \\
&= \mathrm{Sym}\Big\{ \big(\mathcal{I}_3 - \mathcal{L}^- \mathcal{I}_1\big)^T \mathcal{G}^{(1)} \big(\mathcal{L}^+ \mathcal{I}_1 - \mathcal{I}_3\big) \Big\} \\
&\quad + \mathrm{Sym}\Big\{ \big(\mathcal{I}_7 - \mathcal{L}^- \mathcal{I}_6\big)^T \mathcal{G}^{(2)} \big(\mathcal{L}^+ \mathcal{I}_6 - \mathcal{I}_7\big) \Big\}
\end{aligned}$$

and the other notations are given in Theorem 1. Meanwhile, the desired fuzzy time sampled-data controller gains are given as

$$\mathcal{K}_j = \mathcal{M}^{-1} \mathcal{K}_j^*. \tag{45}$$

B. Fuzzy Time–Space Sampled-Data Control for Exponential Synchronization of RDNNs With ATVDs

Dividing $\mho$ into N sampling intervals, we can obtain the space sampling sequence $\underline{\alpha} = x_0 < x_1 < \cdots < x_N = \bar{\alpha}$. The space sampling interval Δ_q satisfies the following condition:

$$\Delta_q \triangleq x_{q+1} - x_q \le \bar{\Delta}, \quad q = 0, 1, \ldots, N-1 \tag{46}$$

where $\bar{\Delta}$ is a positive constant.

Consider the fuzzy time–space sampled-data controller for rule j as follows.

Controller Rule j: IF $\varsigma_1(t)$ is ϑ_1^j and $\ldots$ and $\varsigma_p(t)$ is ϑ_p^j, THEN

$$\begin{aligned}
\mathcal{U}(t,x) &= \mathcal{K}_j \eta\big(t_p, \tilde{x}_q\big), \quad \tilde{x}_q = \frac{x_q + x_{q+1}}{2} \\
&\quad j \in \beth, \ t \in \big[t_p, t_{p+1}\big), \ x \in \big[x_q, x_{q+1}\big)
\end{aligned} \tag{47}$$

where $\mathcal{K}_j \in \mathscr{R}^{n\times n}$ ($j \in \beth$) are the gains to be designed. Then, the overall fuzzy time–space sampled-data controller is represented by

$$\begin{aligned}
\mathcal{U}(t,x) &= \sum_{j=1}^{r} \theta_j\big(\varsigma(t_p)\big) \mathcal{K}_j \eta\big(t_p, \tilde{x}_q\big) \\
&\quad j \in \beth, \ t \in \big[t_p, t_{p+1}\big), \ x \in \big[x_q, x_{q+1}\big).
\end{aligned} \tag{48}$$

Substituting (48) into (4), we have

$$\begin{aligned}
\frac{\partial \eta(t,x)}{\partial t} &= \sum_{m=1}^{r} \sum_{j=1}^{r} \theta_m(\varsigma(t)) \theta_j(\varsigma(t_p)) \\
&\quad \times \Big\{ \mathcal{D} \frac{\partial^2 \eta(t,x)}{\partial x^2} \\
&\qquad - \mathcal{A}_m \eta(t,x) + \mathcal{B}_m^{(1)} \tilde{f}(\eta(t,x)) \\
&\qquad + \mathcal{B}_m^{(2)} \tilde{f}(\eta(t - \varpi_1(t) - \varpi_2(t), x)) \\
&\qquad + \mathcal{K}_j \eta\big(t_p, \tilde{x}_q\big) \Big\} \\
&\quad t \in \big[t_p, t_{p+1}\big), x \in \big[x_q, x_{q+1}\big) \\
\eta\big(t, \underline{\alpha}\big) &= \eta(t, \bar{\alpha}) = 0, \ t \in \big[t_0^*, +\infty\big) \\
\eta\big(s + t_0^*, x\big) &= \phi^*(s,x) \in C\big(\big[-\varpi^*, 0\big] \times \mho, \mathscr{R}^n\big).
\end{aligned} \tag{49}$$

Theorem 2: Let scalars $\varpi_i^* \ge 0$, μ_i ($i = 1, 2$), $h > 0$, $\bar{\Delta}$, and $0 < \delta_1 < 2\kappa < 2\gamma_j$ be given. If there exist symmetric matrices $\mathcal{Z} > 0 \in \mathscr{R}^{n\times n}$, $\mathcal{P} > 0 \in \mathscr{R}^{n\times n}$, $\mathcal{Q}_1 > 0 \in \mathscr{R}^{n\times n}$, $\mathcal{Q}_2 > 0 \in \mathscr{R}^{2n\times 2n}$, $\mathcal{H}_i > 0 \in \mathscr{R}^{n\times n}$ ($i = 1, 2$), $\mathcal{R}_i > 0 \in \mathscr{R}^{n\times n}$ ($i = 1, 2$), $\mathcal{W} > 0 \in \mathscr{R}^{2n\times 2n}$, and $\mathcal{S} = \begin{bmatrix} \mathcal{S}_1 & \mathcal{S}_2 \\ * & \mathcal{S}_3 \end{bmatrix} > 0 \in \mathscr{R}^{2n\times 2n}$, diagonal matrices $\mathcal{G}_{mj}^{(i)} > 0 \in \mathscr{R}^{n\times n}$ ($i = 1, 2$), and any matrices $\mathcal{M} \in \mathscr{R}^{n\times n}$, $\mathcal{Y}_{mj}^{(i)} \in \mathscr{R}^{n\times n}$ ($i = 1, 2, 3$), $\mathcal{F}_{mj} \in \mathscr{R}^{2n\times 4n}$, and $\mathcal{K}_j^* \in \mathscr{R}^{n\times n}$, for any $m, j \in \beth$ satisfying $\mathcal{M}\mathcal{D} \ge 0$, (12)–(14), and

$$\begin{bmatrix} -\delta_1 \mathcal{M}\mathcal{D} & \mathcal{K}_j^{*T} \\ * & -\frac{\pi^2}{\bar{\Delta}^2} \mathcal{Z} \end{bmatrix} < 0 \tag{50}$$

$$\hat{\Psi}(0; h, 0) < 0 \tag{51}$$

$$\begin{bmatrix} \hat{\Psi}(0; h, h) & e^{-2\kappa h} \Upsilon_3^T \mathcal{F}_{mj}^T \\ * & -\frac{1}{h} e^{-2\kappa h} \mathcal{S}_{mj} \end{bmatrix} < 0 \tag{52}$$

then the T–S fuzzy RDNNs (2) and (3) can achieve exponential synchronization under the fuzzy time–space sampled-data controller (48), where $\hat{\Psi}(\varrho; h_p, h(t)) = \sum_{i=1}^{5} \Psi_i(\varrho; h_p, h(t)) + \hat{\Psi}_6(\varrho; h_p, h(t))$ with $\hat{\Psi}_6(\varrho; h_p, h(t)) = \mathrm{Sym}\{(\mathcal{I}_4^T + \gamma_j \mathcal{I}_1^T)\mathcal{M}(-\mathcal{I}_4 - \mathcal{A}_m \mathcal{I}_1 + \mathcal{B}_m^{(1)} \mathcal{I}_3 + \mathcal{B}_m^{(2)} \mathcal{I}_7)\} + \mathrm{Sym}\{(\mathcal{I}_4^T + \gamma_j \mathcal{I}_1^T)\mathcal{K}_j^* \mathcal{I}_2\} - [(2(\gamma_j - \kappa)\pi^2)/((\bar{\alpha} - \underline{\alpha})^2)] \mathcal{I}_1^T \mathcal{M}\mathcal{D}\mathcal{I}_1 + (\mathcal{I}_4 + \gamma_j \mathcal{I}_1)^T \mathcal{Z}(\mathcal{I}_4 + \gamma_j \mathcal{I}_1)$. Furthermore, the fuzzy time–space sampled-data controller gains are given as $\mathcal{K}_j = \mathcal{M}^{-1}\mathcal{K}_j^*$.

Proof: Similar to the proof of Theorem 1, here we only list the different parts. Note that $\eta(t_p, \tilde{x}_q) = \eta(t_p, x) - \int_{\tilde{x}_q}^{x} [(\partial \eta(t_p, \beta))/\partial \beta] d\beta$. For any matrix $\mathcal{M} \in \mathscr{R}^{n\times n}$, one has from system (49) that

$$\begin{aligned}
0 &= 2 \sum_{m=1}^{r} \sum_{j=1}^{r} \theta_m(\varsigma(t)) \theta_j\big(\varsigma(t_p)\big) \sum_{q=0}^{N-1} \int_{x_q}^{x_{q+1}} \Omega^T(t,x) \\
&\quad \times \Bigg[\mathcal{M}\Big(-\frac{\partial \eta(t,x)}{\partial t} + \mathcal{D} \frac{\partial^2 \eta(t,x)}{\partial x^2} - \mathcal{A}_m \eta(t,x) \\
&\qquad + \mathcal{B}_m^{(1)} \tilde{f}(\eta(t,x)) + \mathcal{B}_m^{(2)} \tilde{f}(\eta(t - \varpi(t), x)) \Big) \\
&\qquad + \mathcal{K}_j^* \eta(t_p, x) - \mathcal{K}_j^* \int_{\tilde{x}_q}^{x} \frac{\partial \eta(t_p, \beta)}{\partial \beta} d\beta \Bigg] dx
\end{aligned} \tag{53}$$

where $\Omega(t,x) = (\partial \eta(t,x)/\partial t) + \gamma_j \eta(t,x)$, $\mathcal{K}_j^* = \mathcal{M}\mathcal{K}_j$.

Based on Lemma 2, for any $\mathcal{Z} > 0 \in \mathscr{R}^{n\times n}$, we have from (53) that

$$-2 \sum_{q=0}^{N-1} \int_{x_q}^{x_{q+1}} \Omega^T(t,x) \mathcal{K}_j^* \int_{\tilde{x}_q}^{x} \frac{\partial \eta(t_p, \beta)}{\partial \beta} d\beta dx$$

$$\leq \int_{\underline{\alpha}}^{\bar{\alpha}} \Omega^T(t,x)\mathcal{Z}\Omega(t,x)dx + \sum_{q=0}^{N-1}\left(\int_{x_q}^{\tilde{x}_q} + \int_{\tilde{x}_q}^{x_{q+1}}\right) \times \left[\left(\int_{\tilde{x}_q}^{x} \frac{\partial\eta(t_p,\beta)}{\partial\beta}d\beta\right)^T \mathcal{K}_j^{*T}\mathcal{Z}^{-1}\mathcal{K}_j^* \int_{\tilde{x}_q}^{x} \frac{\partial\eta(t_p,\beta)}{\partial\beta}d\beta\right]dx$$
$$\leq \int_{\underline{\alpha}}^{\bar{\alpha}} \Omega^T(t,x)\mathcal{Z}\Omega(t,x)dx + \frac{\bar{\Delta}^2}{\pi^2}\int_{\underline{\alpha}}^{\bar{\alpha}} \frac{\partial\eta^T(t_p,x)}{\partial x}\mathcal{K}_j^{*T}\mathcal{Z}^{-1}\mathcal{K}_j^*\frac{\partial\eta(t_p,x)}{\partial x}dx. \quad (54)$$

Combining (19)–(33), (35)–(37), (53), and (54), we obtain for $t_p \leq t < t_{p+1}$ that

$$\dot{\mathcal{V}}(t) + 2\kappa\mathcal{V}(t) - \delta_1 \sup_{-\varpi^*\leq s\leq 0}\mathcal{V}(t+s)$$
$$\leq \int_{\underline{\alpha}}^{\bar{\alpha}} \sum_{m=1}^{r}\sum_{j=1}^{r}\theta_m(\varsigma(t))\theta_j(\varsigma(t_p))\zeta^T(t,x) \times \left(\hat{\Psi}(1;h_p,h(t)) + \delta_1\mathcal{I}_2^T\mathcal{P}\mathcal{I}_2\right)\zeta(t,x)dx - \delta_1\mathcal{V}_1(t_p) - \delta_1\mathcal{V}_2(t_p) + \frac{\bar{\Delta}^2}{\pi^2}\sum_{j=1}^{r}\theta_j(\varsigma(t_p)) \times \int_{\underline{\alpha}}^{\bar{\alpha}} \frac{\partial\eta^T(t_p,x)}{\partial x}\mathcal{K}_j^{*T}\mathcal{Z}^{-1}\mathcal{K}_j^*\frac{\partial\eta(t_p,x)}{\partial x}dx$$
$$= \int_{\underline{\alpha}}^{\bar{\alpha}} \sum_{m=1}^{r}\sum_{j=1}^{r}\theta_m(\varsigma(t))\theta_j(\varsigma(t_p))\zeta^T(t,x) \times \hat{\Psi}(1;h_p,h(t))\zeta(t,x)dx + \sum_{j=1}^{r}\theta_j(\varsigma(t_p))\int_{\underline{\alpha}}^{\bar{\alpha}} \frac{\partial\eta^T(t_p,x)}{\partial x} \times \left(-\delta_1\mathcal{M}\mathcal{D} + \frac{\bar{\Delta}^2}{\pi^2}\mathcal{K}_j^{*T}\mathcal{Z}^{-1}\mathcal{K}_j^*\right)\frac{\partial\eta(t_p,x)}{\partial x}dx. \quad (55)$$

Then, using the Schur complement to (50) and (52), from Lemma 3, (51), and (55), the T–S fuzzy RDNNs (2) and (3) can achieve exponential synchronization under the fuzzy time–space sampled-data controller (48). The proof is completed.■

Remark 5: By sampling the time t, we design the time sampled-data controller (7). Note that the state vector $\varphi(t,x)$ of RDNN (1) is related to both time t and space x. When sampling both t and x, we design the time–space sampled-data controller (48). Compared with time sampled-data controller (7), the time–space sampled-data controller (48) uses less sampling signals, which can further save the communication resources of RDNNs.

Remark 6: In LMI-based conditions, the number of decision variables (NDVs) and the dimensions of the LMIs are two key factors for computational complexity [40]. In general, NDV is used as an index of computational complexity. By computation, the NDVs of the fuzzy time sampled-data control approach in Theorem 1 and the fuzzy time–space sampled-data control approach in Theorem 2 are $11n^2r^2+n^2r+2nr^2+10n^2+6n$ and $11n^2r^2+n^2r+2nr^2+10.5n^2+6.5n$, respectively. Note that in order to derive less conservative synchronization criteria, the fuzzy-dependent adjustable matrix inequality technique in Lemma 4 is used to estimate the derivative of the constructed LKF (18). By introducing more adjustable matrices, the conservatism of the obtained synchronization criteria can effectively be reduced, which will be verified in the next section. The limitation of the fuzzy-dependent adjustable matrix inequality technique is that it reduces the conservatism but increases the NDVs, which will increase the computational complexity to some extent. How to weigh the conservatism and computational complexity will be considered in our future work.

Algorithm 1 MASP Search Algorithm

Step 1: For given $0 < \delta_1 < \kappa < 2\gamma_j (j = 1, 2, \ldots, r)$, specify the ranges h with increments $\Delta h > 0$. Set $h = \Delta h$.

Step 2: Use MATLAB LMI Toolbox to solve LMIs in Theorem 1 with specified h.

Step 3: If there exists a feasible solution, then let $h = h+\Delta h$, and go to Step 2. Otherwise, go to Step 4.

Step 4: If $h = \Delta h$, output "No feasible solution satisfying Theorem 1." Then reselect values of $0 < \delta_1 < \kappa < 2\gamma_j (j = 1, 2, \ldots, r)$, go to Step 1. Otherwise, go to Step 5.

Step 5: Output $h = h - \Delta h$, which is the MASP. With the output MASP h, and using MATLAB LMI Toolbox to solve the LMIs in Theorem 1, we obtain the corresponding feasible matrices. Then, from (17), we find the controller gains $\mathcal{K}_j (j = 1, 2, \ldots, r)$.

IV. Simulation Examples

In this section, some simulations are presented to verify the effectiveness and superiority of the theoretical results. In order to show how the theory results from the previous sections are applied in this section, Algorithm 1 is given to find the maximum-allowable sampling period (MASP) h and controller gains $\mathcal{K}_j (j = 1, 2, \ldots, r)$.

Example 1: Consider the T–S fuzzy RDNN (1) with the membership functions $\theta_1(\varsigma(t)) = \frac{1}{2}(1+\sin t)$ and $\theta_2(\varsigma(t)) = \frac{1}{2}(1-\sin t)$ for rules 1 and 2, respectively, and the following parameters:

$$\mathcal{A}_1 = \begin{bmatrix}1 & 0\\ 0 & 1\end{bmatrix},\quad \mathcal{B}_1^{(1)} = \begin{bmatrix}2 & -0.1\\ -5 & 3\end{bmatrix}$$
$$\mathcal{B}_1^{(2)} = \begin{bmatrix}-1.5 & -0.1\\ -0.2 & -2.5\end{bmatrix},\quad \mathcal{A}_2 = \begin{bmatrix}1.2 & 0\\ 0 & 1.2\end{bmatrix}$$
$$\mathcal{B}_2^{(1)} = \begin{bmatrix}3.6 & -0.4\\ -8 & 8\end{bmatrix},\quad \mathcal{B}_2^{(2)} = \begin{bmatrix}-3.6 & -0.24\\ -0.6 & -6\end{bmatrix}$$
$$\mathcal{D} = \begin{bmatrix}0.6 & 0\\ 0 & 0.6\end{bmatrix},\quad \mho = \{x| -1 \leq x \leq 5\},$$
$$\varpi_1(t) = |\sin(0.1t)|,\quad \varpi_2(t) = |\cos(0.1t)|$$
$$\urcorner(t) = 0,\quad f_i(\vartheta_i(t,x)) = \tanh(\varphi_i(t,x))\ (i = 1, 2)$$

from which we obtain $\varpi_i^* = 1$, $\mu_i = 0.1$ $(i = 1, 2)$, $l_1^- = l_2^- = 0$, and $l_1^+ = l_2^+ = 1$. Take the initial conditions of the drive system (1) as $\phi_1(s,x) = 1.5\upsilon(x)$ and $\phi_2(s,x) = -2\upsilon(x)$, and the response system (3) as $\tilde{\phi}_1(s,x) = 1.425\upsilon(x)$ and $\tilde{\phi}_2(s,x) = -2.1\upsilon(x)$, where $\upsilon(x) = \cos([\pi(x-2)]/6)$.

Next, we shall discuss the following two cases.

Case 1: Fuzzy time sampled-data control for exponential synchronization of RDNNs (2) and (3).

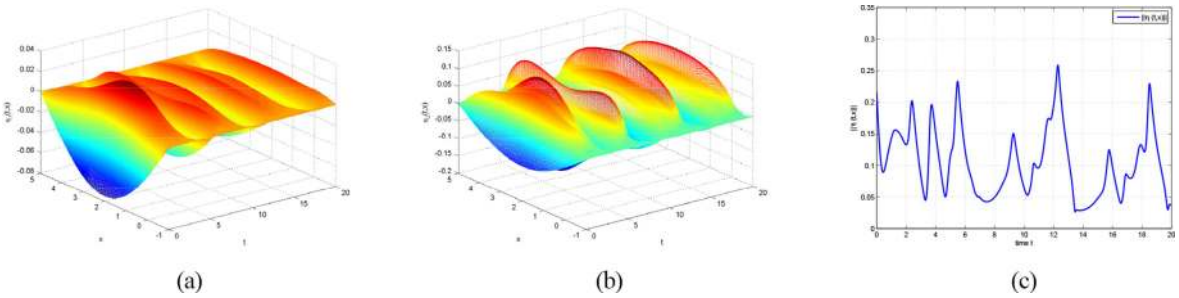

Fig. 1. Trajectories of states with $\mathcal{U}(t,x)=0$. (a) $\eta_1(t,x)$. (b) $\eta_2(t,x)$. (c) $\|\eta(t,x)\|$.

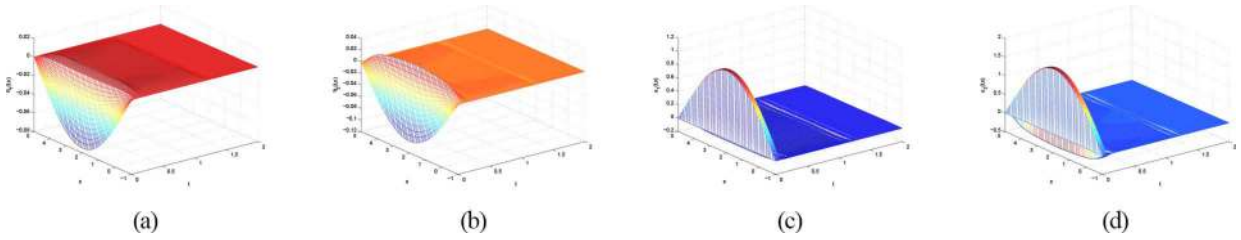

Fig. 2. Trajectories of controlled states and the corresponding fuzzy time sampled-data controller (7). (a) $\eta_1(t,x)$. (b) $\eta_2(t,x)$. (c) $\mathcal{U}_1(t,x)$. (d) $\mathcal{U}_2(t,x)$.

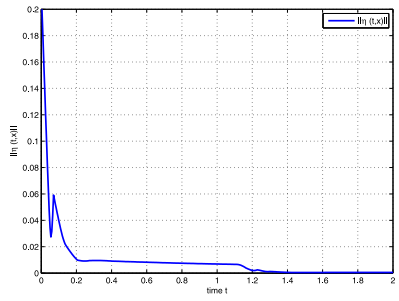

Fig. 3. Evolution of $\|\eta(t,x)\|$ with fuzzy time sampled-data controller (7).

Case 2: Fuzzy time–space sampled-data control for exponential synchronization of RDNNs (2) and (3).

When $\mathcal{U}(t,x)=0$, the trajectories of states $\eta_i(t,x)$ $(i=1,2)$ and $\|\eta(t,x)\|$ are depicted in Fig. 1. From Fig. 1, we find the synchronization of drive–response systems (2) and (3) cannot be realized if there is no control input.

For Case 1: We first verify the effectiveness of Theorem 1. Choosing $\kappa=0.03$, $\delta_1=0.04$, $\gamma_1=7$, and $\gamma_2=9$, by Algorithm 1, we can find the MASP $h=0.0683$. The corresponding fuzzy time sampled-data controller gains are $\mathcal{K}_1=\begin{bmatrix}-14.9429 & 0.3877\\ 0.2703 & -17.8713\end{bmatrix}$ and $\mathcal{K}_2=\begin{bmatrix}-13.4753 & 0.3461\\ 0.2506 & -17.3788\end{bmatrix}$. With the above controller gains, Fig. 2 shows the controlled trajectories of states $\eta_i(t,x)$ $(i=1,2)$ and the corresponding fuzzy time sampled-data controller (7). The evolution of the controlled $\|\eta(t,x)\|$ is plotted in Fig. 3. From Fig. 3, one finds the exponential synchronization of the drive–response systems (2) and (3) is realized, which illustrates the effectiveness of Theorem 1 and the fuzzy time sampled-data controller (7).

Then, we show the superiority of the fuzzy-dependent adjustable matrix approach. For various κ, the MASPs h by Theorem 1 and Corollary 1 are given in Table I. From Table I,

TABLE I
MASP h FOR VARIOUS κ IN CASE 1

κ	0.03	0.05	0.07	0.1	0.2
Theorem 1	0.0683	0.0663	0.0643	0.0613	0.0512
Corollary 1	0.0564	0.0549	0.0535	0.0513	0.0439

we find, for various κ, the MASPs h by Theorem 1 are all bigger than those by Corollary 1. It is noted that Theorem 1 is obtained by the fuzzy-dependent adjustable matrix approach, and Corollary 1 is obtained by the traditional estimation technique in Lemma 1 [35]. Thus, compared with the traditional estimation technique in Lemma 1 [35], the fuzzy-dependent adjustable matrix approach is more effective to reduce the conservatism.

For Case 2: Take $\kappa=0.35$, $\delta_1=0.6799$, $\bar{\Delta}=0.06$, $\gamma_1=15$, and $\gamma_2=16$. By Theorem 2, one obtains the MASP $h=0.0206$ and the fuzzy time–space sampled-data controller gains as $\mathcal{K}_1=\begin{bmatrix}-21.4595 & 0.1697\\ 0.5273 & -27.5542\end{bmatrix}$ and $\mathcal{K}_2=\begin{bmatrix}-21.6003 & 0.1625\\ 0.8195 & -27.5568\end{bmatrix}$. With the above parameters, the trajectories of states $\eta_i(t,x)$ $(i=1,2)$ and the corresponding fuzzy time–space sampled-data controller (48) are displayed in Fig. 4. Fig. 5 displays the evolution of the error signal $\|\eta(t,x)\|$. From Fig. 5, it is clear that the trajectory of $\|\eta(t,x)\|$ converges to zero, which shows the effectiveness of Theorem 2 and the fuzzy time–space sampled-data controller (48).

Example 2: This example presents the application of the obtained results to image encryption, which is based on the following algorithm.

Consider the T–S fuzzy RDNN (1) with the following parameters:

$$\mathcal{A}_1=I_3,\ \mathcal{B}_1^{(1)}=\begin{bmatrix}1+\frac{\pi}{4} & 20 & 0.001\\ 0.1 & 1+\frac{\pi}{4} & 0.001\\ 3 & -0.56 & -0.12\end{bmatrix}$$

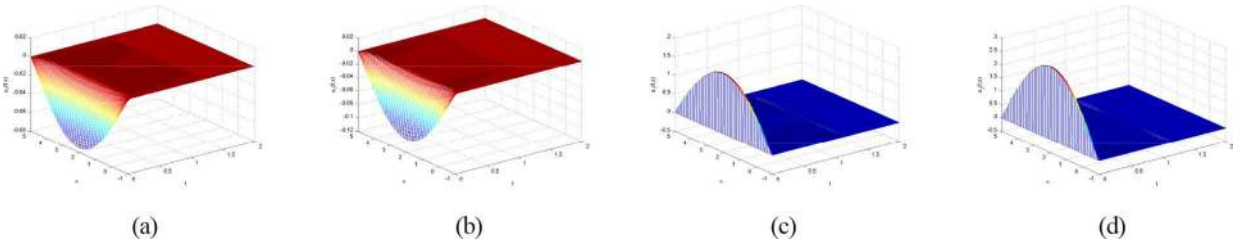

Fig. 4. Trajectories of states $\eta_i(t,x)$ $(i=1,2)$ and the corresponding fuzzy time–space sampled-data controller (48). (a) $\eta_1(t,x)$. (b) $\eta_2(t,x)$. (c) $\mathcal{U}_1(t,x)$. (d) $\mathcal{U}_2(t,x)$.

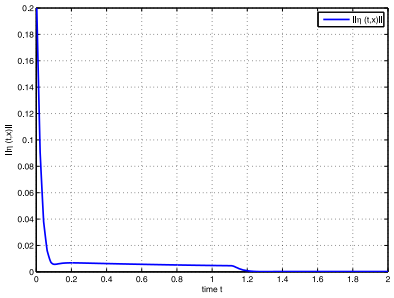

Fig. 5. Evolution of error signal $\|\eta(t,x)\|$ with fuzzy time–space sampled-data controller (48).

$$\mathcal{A}_2=\frac{1}{2}I_3,\ \mathcal{B}_1^{(2)}=\begin{bmatrix}-1.3\sqrt{2}\frac{\pi}{4} & 0.1 & -0.001\\ 0.1 & -1.3\sqrt{2}\frac{\pi}{4} & 0.01\\ 2 & -0.85 & 0.02\end{bmatrix}$$

$$\mathcal{B}_2^{(1)}=\begin{bmatrix}2+\frac{\pi}{2} & 40 & 0.002\\ 0.2 & 2+\frac{\pi}{2} & 0.002\\ 6 & -1.12 & -0.24\end{bmatrix},\ \mathcal{D}=10^{-4}I_3$$

$$\mathcal{B}_2^{(2)}=\begin{bmatrix}-1.3\sqrt{2}\frac{\pi}{8} & 0.05 & -0.0005\\ 0.05 & -1.3\sqrt{2}\frac{\pi}{8} & 0.005\\ 1 & -0.425 & 0.01\end{bmatrix}$$

$$\varpi_1(t)=0.4,\ \varpi_2(t)=0.5,\ \mho=\{x|-0.5\le x\le 0.5\}$$

$$\theta_1(\varsigma(t))=1-0.1\sin^2 t,\ \theta_2(\varsigma(t))=0.1\sin^2 t,\ \urcorner(t)=0$$

and $f_i(\vartheta_i(t,x))=[(|\varphi_i(t,x)+1|-|\varphi_i(t,x)-1|)/2]$ $(i=1,2,3)$, from which one has $l_i^-=0, l_i^+=1$ $(i=1,2,3)$. Take the initial conditions of the drive system (1) as $\phi_1(s,x)=1.5\upsilon(x)$, $\phi_2(s,x)=-2\upsilon(x)$, and $\phi_3(s,x)=0.5\upsilon(x)$, and the response system (3) as $\tilde{\phi}_1(s,x)=1.425\upsilon(x)$, $\tilde{\phi}_2(s,x)=-3\upsilon(x)$, and $\tilde{\phi}_3(s,x)=0.55\upsilon(x)$, where $\upsilon(x)=\cos(\pi x)$.

The drive system (1) exhibits chaotic behavior as shown in Fig. 6.

Taking $\kappa=0.03$, $\delta_1=0.04$, $\gamma_1=7$, and $\gamma_2=9$, by Theorem 1, we find the MASP $h=0.1578$. The corresponding controller gains are

$$\mathcal{K}_1=\begin{bmatrix}-7.1702 & -16.2038 & 0.3703\\ -0.0846 & -7.3688 & -0.0247\\ -2.8976 & -21.2411 & -4.7118\end{bmatrix}$$

and

$$\mathcal{K}_2=\begin{bmatrix}-6.3356 & -17.3634 & 0.4061\\ -0.0722 & -6.4514 & -0.0259\\ -2.1958 & -21.9220 & -4.1847\end{bmatrix}.$$

Algorithm 2 Image Encryption and Decryption Algorithm Based on Fuzzy Sampled-Data Synchronization

Step 1: Process the original image. Read the pixel values of the original image with size $m\times n$. The pixel value is denoted by p_{ij} $(i=1,2,\ldots,m,\ j=1,2,\ldots,n)$.

Step 2: Generate a chaotic sequence by the drive system after time t_b, where t_b is the time after the synchronization realized. Select $\bar{m}$ instants of time $t_b\le\bar{t}_1<\bar{t}_2<\cdots<\bar{t}_{\bar{m}}$ and $\bar{n}$ spatial points $\underline{\alpha}\le\bar{x}_1<\bar{x}_2<\cdots<\bar{x}_{\bar{n}}\le\bar{\alpha}$ such that $\bar{m}\times\bar{n}=m\times n$. Then the data $\varphi(\bar{t}_i,\bar{x}_j)$ $(i=1,2,\ldots,\bar{m},\ j=1,2,\ldots,\bar{n})$ is the generated chaotic sequence. Reshape the chaotic sequence to a matrix with size $m\times n$. The matrix elements are denoted by c_{ij} $(i=1,2,\ldots,m,\ j=1,2,\ldots,n)$.

Step 3: The encrypted signals are derived as follows:

$$e_{ij}=\mod([\|c_{ij}\|\times 10^8],256)\oplus p_{ij}$$

where $\oplus$ is the XOR operation.

Step 4: The encrypted image is derived by writing the e_{ij} $(i=1,2,\ldots,m,\ j=1,2,\ldots,n)$.

The decryption process is the reverse of the encryption process, which is omitted here.

With the above controller gains, Fig. 7 shows the controlled trajectories of states $\eta_i(t,x)$ $(i=1,2,3)$. From Fig. 7, we find the synchronization between systems (2) and (3) is achieved.

Then, according to Algorithm 2, the Lena grayscale original image, encrypted image, and decrypted image are shown in Fig. 8(a), and their corresponding histograms are given in Fig. 8(b). From Fig. 8, one finds that our obtained results can successfully solve the image encryption problem of secure communication.

V. Conclusion

In this article, we have studied the exponential synchronization problem of T–S fuzzy RDNNs with ATVDs. By proposing the fuzzy time and time–space sampled-data control schemes, and the fuzzy-dependent adjustable matrix inequality technique, and constructing the suitable LKF, we have obtained some new exponential synchronization criteria for T–S fuzzy RDNNs with ATVDs. The two fuzzy sampled-data control schemes are more applicable since they cannot only tolerate some uncertainties but also save the limited communication resources for T–S fuzzy RDNNs with ATVDs. The fuzzy-dependent adjustable matrix inequality technique was first proposed. Compared with some traditional estimation

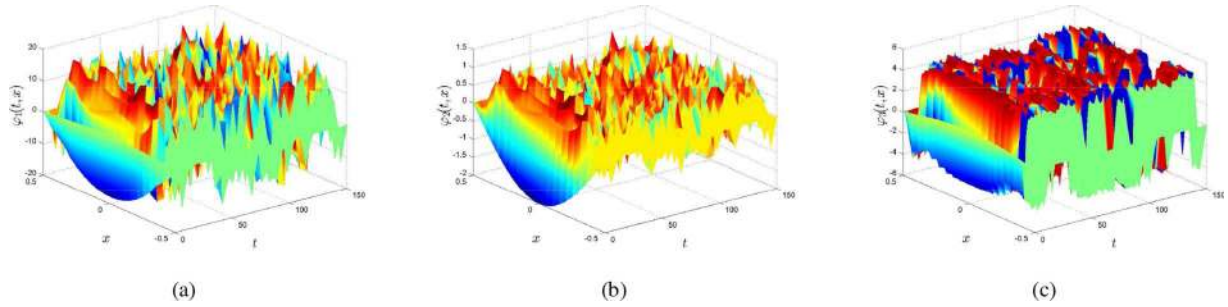

(a) (b) (c)

Fig. 6. Chaotic behavior of system (1). (a) $\varphi_1(t,x)$. (b) $\varphi_2(t,x)$. (c) $\varphi_3(t,x)$.

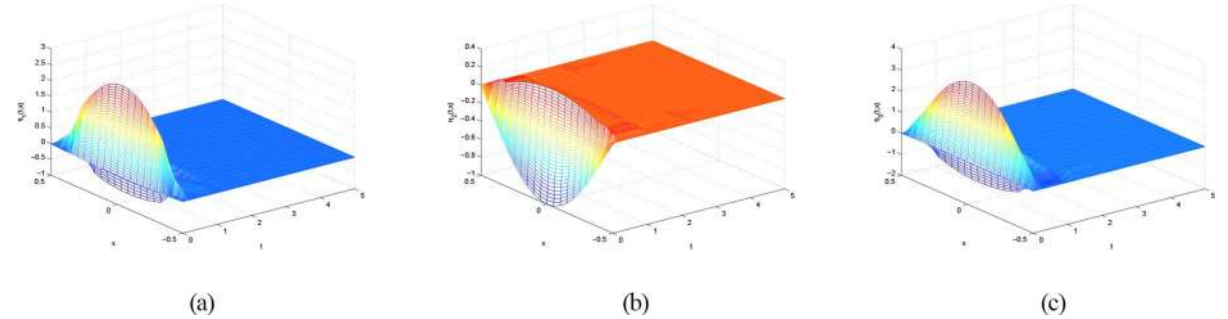

(a) (b) (c)

Fig. 7. Trajectories of controlled states. (a) $\eta_1(t,x)$. (b) $\eta_2(t,x)$. (c) $\eta_3(t,x)$.

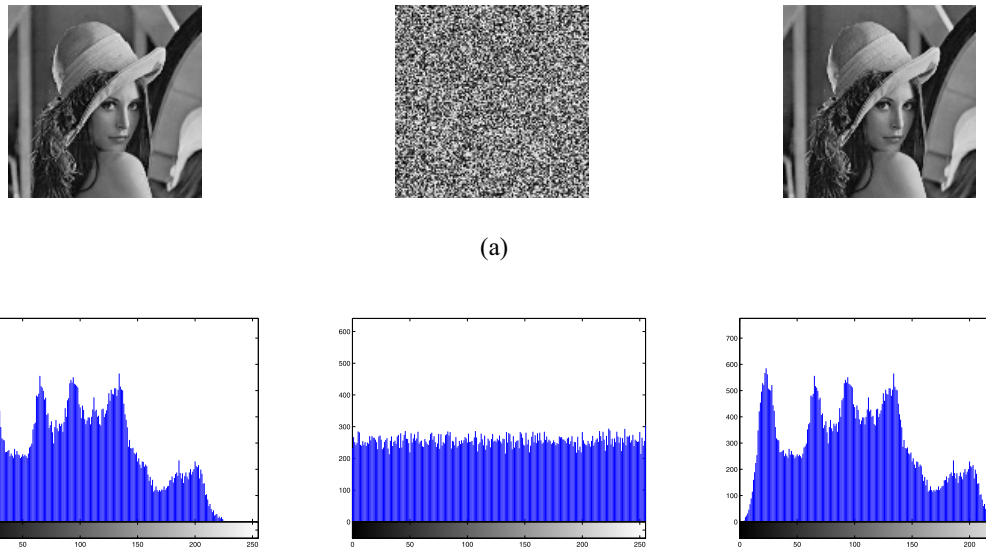

(a)

(b)

Fig. 8. (a) *Lena* grayscale original image, encrypted image, and decrypted image and (b) their corresponding histograms.

techniques with a determined constant matrix, the fuzzy-dependent adjustable matrix approach is more flexible and helpful to reduce the conservatism. Finally, we have discussed some simulations to verify the effectiveness and superiority of the obtained theoretical results. It is noted that a new time-dependent fuzzy LKF approach has been proposed in [41], which can effectively capture the information of membership functions. In our future work, the time-dependent fuzzy LKF approach will be considered for T–S fuzzy RDNNs and the fuzzy-dependent adjustable matrix inequality technique can be extended to other T–S fuzzy systems.

REFERENCES

[1] L. Wang and H.-K. Lam, "New stability criterion for continuous-time Takagi–Sugeno fuzzy systems with time-varying delay," *IEEE Trans. Cybern.*, vol. 49, no. 4, pp. 1551–1556, Apr. 2019.

[2] H. K. Lam, "A review on stability analysis of continuous-time fuzzy-model-based control systems: From membership-function-independent to membership-function-dependent analysis," *Eng. Appl. Artif. Intel.*, vol. 67, pp. 390–408, Jan. 2018.

[3] J. Cheng, Y. Shan, J. Cao, and J. H. Park, "Nonstationary control for T-S fuzzy Markovian switching systems with variable quantization density," *IEEE Trans. Fuzzy Syst.*, early access, Feb. 17, 2020, doi: 10.1109/TFUZZ.2020.2974440.

[4] C.-F. Juang, M.-G. Lai, and W.-T. Zeng, "Evolutionary fuzzy control and navigation for two wheeled robots cooperatively carrying an object in unknown environments," *IEEE Trans. Cybern.*, vol. 45, no. 9, pp. 1731–1743, Sep. 2015.

[5] R.-E. Precup, M.-L. Tomescu, and C.-A. Dragos, "Stabilization of Rössler chaotic dynamical system using fuzzy logic control algorithm," *Int. J. Gen. Syst.*, vol. 43, no. 5, pp. 413–433, 2014.

[6] R. P. A. Gil, Z. C. Johanyák, and T. Kovács, "Surrogate model based optimization of traffic lights cycles and green period ratios using microscopic simulation and fuzzy rule interpolation," *Int. J. Artif. Intell.*, vol. 16, no. 1, pp. 20–40, Apr. 2018.

[7] Z. Zhang, H. Liang, C. Wu, and C. K. Ahn, "Adaptive event-triggered output feedback fuzzy control for nonlinear networked systems with packet dropouts and actuator failure," *IEEE Trans. Fuzzy Syst.*, vol. 27, no. 9, pp. 1793–1806, Sep. 2019.

[8] H. Zhang, Y. Wang, and D. Liu, "Delay-dependent guaranteed cost control for uncertain stochastic fuzzy systems with multiple time delays," *IEEE Trans. Syst., Man, Cybern. B, Cybern.*, vol. 38, no. 1, pp. 126–140, Feb. 2008.

[9] P. Selvaraj, R. Sakthivel, and H. R. Karimi, "Equivalent-input-disturbance-based repetitive tracking control for Takagi–Sugeno fuzzy systems with saturating actuator," *IET Control Theory Appl.*, vol. 10, no. 15, pp. 1916–1927, Oct. 2016.

[10] Z. G. Wu, P. Shi, H. Su, and R. Lu, "Dissipativity-based sampled-data fuzzy control design and its application to truck–trailer system," *IEEE Trans. Fuzzy Syst.*, vol. 23, no. 5, pp. 1669–1679, Oct. 2015.

[11] T. Li, Z. Dai, G. Song, L. Wang, and H. Du, "Fault tolerant tracking of Mars entry vehicles via fuzzy control approach," *Fuzzy Sets Syst.*, vol. 371, pp. 123–135, Sep. 2019.

[12] A. Cochocki and R. Unbehauen, *Neural Networks for Optimization and Signal Processing*. Hoboken, NJ, USA: Wiley, 1993.

[13] J. Xiao and S. Zhong, "Extended dissipative conditions for memristive neural networks with multiple time delays," *Appl. Math. Comput.*, vol. 323, pp. 145–163, Apr. 2018.

[14] J. H. Park, H. Shen, X.-H. Chang, and T. H. Lee, *Recent Advances in Control and Filtering of Dynamic Systems With Constrained Signals*. Cham, Switzerland: Springer, 2018.

[15] W. Xie, H. Zhu, J. Cheng, S. Zhong, and K. Shi, "Finite-time asynchronous H_∞ resilient filtering for switched delayed neural networks with memory unideal measurements," *Inf. Sci.*, vol. 487, pp. 156–175, Jun. 2019.

[16] L. M. Pecora and T. L. Carroll, "Synchronization in chaotic systems," *Phys. Rev. Lett.*, vol. 64, no. 8, pp. 821–824, 1990.

[17] R. Zhang, D. Zeng, J. H. Park, Y. Liu, and S. Zhong, "Quantized sampled-data control for synchronization of inertial neural networks with heterogeneous time-varying delays," *IEEE Trans. Neural Netw. Learn. Syst.*, vol. 29, no. 12, pp. 6385–6395, Dec. 2018.

[18] V. Milanović and M. E. Zaghloul, "Synchronization of chaotic neural networks and applications to communications," *Int. J. Bifurcation Chaos*, vol. 6, no. 12, pp. 2571–2585, Dec. 1996.

[19] W. H. Chen, S. Luo, and W. X. Zheng, "Impulsive synchronization of reaction–diffusion neural networks with mixed delays and its application to image encryption," *IEEE Trans. Neural Netw. Learn. Syst.*, vol. 27, no. 12, pp. 2696–2710, Dec. 2016.

[20] D. Zeng, Z. Pu, R. Zhang, S. Zhong, Y. Liu, and G.-C. Wu, "Stochastic reliable synchronization for coupled Markovian reaction–diffusion neural networks with actuator failures and generalized switching policies," *Appl. Math. Comput.*, vol. 357, pp. 88–106, Sep. 2019.

[21] J. L. Wang, X.-X. Zhang, H. N. Wu, T. Huang, and Q. Wang, "Finite-time passivity and synchronization of coupled reaction–diffusion neural networks with multiple weights," *IEEE Trans. Cybern.*, vol. 49, no. 9, pp. 3385–3397, Sep. 2019.

[22] X. Liu, K. Zhang, and W. C. Xie, "Pinning impulsive synchronization of reaction–diffusion neural networks with time-varying delays," *IEEE Trans. Neural Netw. Learn. Syst.*, vol. 28, no. 5, pp. 1055–1067, May 2017.

[23] L. Wang, H. He, Z. Zeng, and C. Hu, "Global stabilization of fuzzy memristor-based reaction–diffusion neural networks," *IEEE Trans. Cybern.*, early access, Nov. 13, 2019, doi: 10.1109/TCYB.2019.2949468.

[24] X. Yang, Q. Song, J. Cao, and J. Lu, "Synchronization of coupled Markovian reaction–diffusion neural networks with proportional delays via quantized control," *IEEE Trans. Neural Netw. Learn. Syst.*, vol. 30, no. 3, pp. 951–958, Mar. 2019.

[25] X. Xie, X. Liu, H. Xu, X. Luo, and G. Liu, "Synchronization of coupled reaction–diffusion neural networks: Delay-dependent pinning impulsive control," *Commun. Nonlinear Sci. Numer. Simul.*, vol. 79, Dec. 2019, Art. no. 104905.

[26] L. Shanmugam, P. Mani, R. Rajan, and Y. H. Joo, "Adaptive synchronization of reaction–diffusion neural networks and its application to secure communication," *IEEE Trans. Cybern.*, vol. 50, no. 3, pp. 911–922, Mar. 2020.

[27] H. K. Lam and F. H. F. Leung, "Design and stabilization of sampled-data neural-network-based control systems," *IEEE Trans. Syst., Man, Cybern. B, Cybern.*, vol. 36, no. 5, pp. 995–1005, Oct. 2006.

[28] R. Zhang, D. Zeng, J. H. Park, H.-K. Lam, and S. Zhong, "Fuzzy adaptive event-triggered sampled-data control for stabilization of T-S fuzzy memristive neural networks with reaction–diffusion terms," *IEEE Trans. Fuzzy Syst.*, early access, Apr. 06, 2020, doi: 10.1109/TFUZZ.2020.2985334.

[29] E. Fridman, "A refined input delay approach to sampled-data control," *Automatica*, vol. 26, no. 2, pp. 421–427, Feb. 2010.

[30] D. Zeng, R. Zhang, J. H. Park, Z. Pu, and Y. Liu, "Pinning synchronization of directed coupled reaction–diffusion neural networks with sampled-data communications," *IEEE Trans. Neural Netw. Learn. Syst.*, early access, Aug. 05, 2019, doi: 10.1109/TNNLS.2019.2928039.

[31] B. Lu, H. Jiang, C. Hu, and A. Abdurahman, "Synchronization of hybrid coupled reaction–diffusion neural networks with time delays via generalized intermittent control with spacial sampled-data," *Neural Netw.*, vol. 105, pp. 75–87, Sep. 2018.

[32] S. Chen, C.-C. Lim, P. Shi, and Z. Lu, "Synchronization control for reaction–diffusion FitzHugh–Nagumo systems with spatial sampled-data," *Automatica*, vol. 93, pp. 352–362, Jul. 2018.

[33] R. Rakkiyappan, S. Dharani, and Q. Zhu, "Synchronization of reaction–diffusion neural networks with time-varying delays via stochastic sampled-data controller," *Nonlinear Dyn.*, vol. 79, no. 1, pp. 485–500, Jan. 2015.

[34] H. K. Lam and F. H. F. Leung, "Sampled-data fuzzy controller for time-delay nonlinear systems: Fuzzy-model-based LMI approach," *IEEE Trans. Syst., Man, Cybern. B, Cybern.*, vol. 37, no. 3, pp. 617–629, Jun. 2007.

[35] H. Zhang, J. Wang, Z. Wang, and H. Liang, "Sampled-data synchronization analysis of Markovian neural networks with generally incomplete transition rates," *IEEE Trans. Neural Netw. Learn. Syst.*, vol. 28, no. 3, pp. 740–752, Mar. 2017.

[36] G. H. Hardy, J. E. Littlewood, and G. Pólya, *Inequalities*. Cambridge, U.K.: Cambridge University Press, 1988.

[37] A. Halanay, *Differential Equations: Stability, Oscillations, Time Lags*. New York, NY, USA: Academic, 1966.

[38] K. Gu, "An integral inequality in the stability problem of time-delay systems," in *Proc. 39th IEEE Conf. Decis. Control*, Sydney, NSW, Australia, 2000, pp. 2805–2810.

[39] P. G. Park, J. W. Ko, and C. Jeong, "Reciprocally convex approach to stability of systems with time-varying delays," *Automatica*, vol. 47, no. 1, pp. 235–238, Jan. 2011.

[40] Y. Li, K. Gu, J. Zhou, and S. Xu, "Estimating stable delay intervals with a discretized Lyapunov–Krasovskii functional formulation," *Automatica*, vol. 50, no. 6, pp. 1691–1697, Jun. 2014.

[41] H. S. Kim, J. B. Park, and Y. H. Joo, "A fuzzy Lyapunov–Krasovskii functional approach to sampled-data output-feedback stabilization of polynomial fuzzy systems," *IEEE Trans. Fuzzy Syst.*, vol. 26, no. 1, pp. 366–373, Feb. 2018.

Ruimei Zhang received the Ph.D. degree in applied mathematics from the School of Mathematical Sciences, University of Electronic Science and Technology of China, Chengdu, China, in 2019.

In 2020, she joined the College of Cybersecurity, Sichuan University, Chengdu, where she is currently a Distinguished Associate Research Fellow. From 2017 to 2018, she was a Visiting Scholar with the Department of Applied Mathematics, University of Waterloo, Waterloo, ON, Canada. From 2018 to 2019, she was a Visiting Scholar with the Department of Electrical Engineering, Yeungnam University, Gyeongsan, South Korea. Her current research interests include memristive neural networks, chaotic Lur'e systems, and synchronization or stability of control systems with delay.

Deqiang Zeng was born in Yibin, China. He received the B.S. degree in mathematics and applied mathematics from Sichuan Normal University, Chengdu, China, where he is currently pursuing the Ph.D. degree.

He is also a Professor with the College of Mathematics and Information Science, Neijiang Normal University, Neijiang, China. His current research interests include sampled-data control, synchronization, reaction–diffusion systems, stochastic Markov jump, and complex networks systems.

Ju H. Park (Senior Member, IEEE) received the Ph.D. degree in electronics and electrical engineering from the Pohang University of Science and Technology (POSTECH), Pohang, South Korea, in 1997.

From 1997 to 2000, he was a Research Associate with the Engineering Research Center-Automation Research Center, POSTECH. In 2000, he joined Yeungnam University, Gyeongsan, South Korea, where he is currently the Chuma Chair Professor. He has coauthored the *Monographs: Recent Advances in Control and Filtering of Dynamic Systems With Constrained Signals* (New York, NY, USA: Springer-Nature, 2018) and *Dynamic Systems With Time Delays: Stability and Control* (New York, NY, USA: Springer-Nature, 2019). He is the editor of an edited volume: *Recent Advances in Control Problems of Dynamical Systems and Networks* (New York, NY, USA: Springer-Nature, 2020). His research interests include robust control and filtering, neural/complex networks, fuzzy systems, multiagent systems, and chaotic systems. He has published a number of papers in these areas.

Prof. Park has been a recipient of the Highly Cited Researcher Award by Clarivate Analytics (formerly, Thomson Reuters) since 2015 and listed in three fields: engineering, computer sciences, and mathematics in 2019. He serves as an Editor for the *International Journal of Control, Automation and Systems*. He is also a Subject Editor/Advisory Editor/Associate Editor/Editorial Board Member for several international journals, including *IET Control Theory and Applications*, *Applied Mathematics and Computation*, the *Journal of The Franklin Institute*, *Nonlinear Dynamics*, *Engineering Reports*, *Cogent Engineering*, the IEEE TRANSACTIONS ON FUZZY SYSTEMS, the IEEE TRANSACTIONS ON NEURAL NETWORKS AND LEARNING SYSTEMS, and the IEEE TRANSACTIONS ON CYBERNETICS. He is a Fellow of the Korean Academy of Science and Technology.

Hak-Keung Lam (Fellow, IEEE) received the B.Eng. (Hons.) and Ph.D. degrees from the Department of Electronic and Information Engineering, Hong Kong Polytechnic University, Hong Kong, in 1995 and 2000, respectively.

From 2000 to 2005, he worked with the Department of Electronic and Information Engineering, Hong Kong Polytechnic University, as a Postdoctoral Fellow and a Research Fellow, respectively. In 2005, he joined as a Lecturer with King's College London, London, U.K., where he is currently a Reader. He has authored/coauthored three monographs: *Stability Analysis of Fuzzy-Model-Based Control Systems* (Springer, 2011), *Polynomial Fuzzy Model Based Control Systems* (Springer, 2016), and *Analysis and Synthesis for Interval Type-2 Fuzzy-Model-Based Systems* (Springer, 2016). His current research interests include intelligent control, computational intelligence, and machine learning.

Dr. Lam has served as a program committee member, international advisory board member, invited session chair, and the publication chair for various international conferences and a reviewer for various books, international journals, and international conferences. He is a Co-Editor of two edited volumes: *Control of Chaotic Nonlinear Circuits* (World Scientific, 2009) and *Computational Intelligence and Its Applications* (World Scientific, 2012). He is an Associate Editor of the IEEE TRANSACTIONS ON FUZZY SYSTEMS, the IEEE TRANSACTIONS ON CIRCUITS AND SYSTEMS— PART II: EXPRESS BRIEFS, *IET Control Theory and Applications*, the *International Journal of Fuzzy Systems*, *Neurocomputing*, and *Nonlinear Dynamics*; and a Guest Editor and on the editorial board for a number of international journals. He was named as a Highly Cited Researcher.

Xiangpeng Xie (Member, IEEE) received the B.S. and Ph.D. degrees in engineering from Northeastern University, Shenyang, China, in 2004 and 2010, respectively.

From 2010 to 2014, he was a Senior Engineer with the Metallurgical Corporation of China Ltd., Beijing, China. He is currently a Professor with the Institute of Advanced Technology, Nanjing University of Posts and Telecommunications, Nanjing, China. His research interests include fuzzy modeling and control synthesis, state estimations, optimization in process industries, and intelligent optimization algorithms.

Prof. Xie serves as an Associate Editor for the *International Journal of Control, Automation, and Systems* and the *International Journal of Fuzzy Systems*.